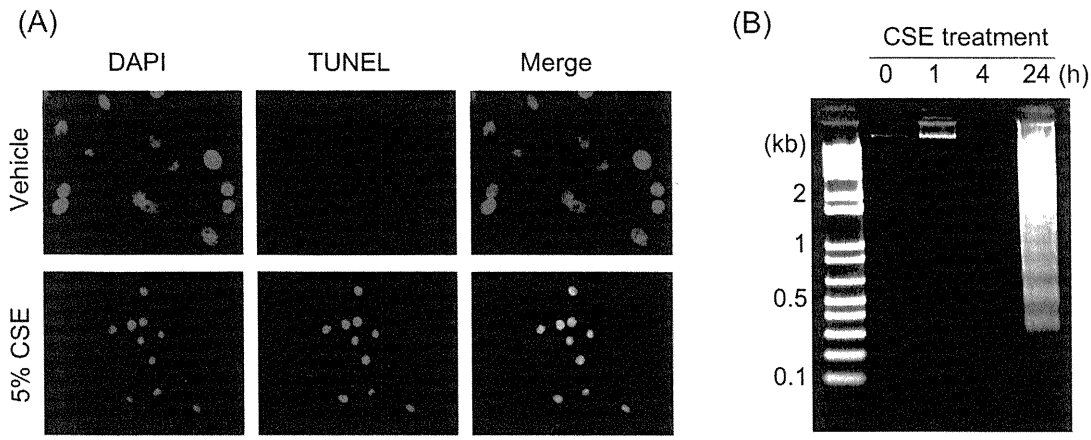

Fig. 5. CSE induces DNA fragmentation in C6 glioma cells as determined by TUNEL staining (A) or agarose gel electrophoresis (B). After C6 glioma cells were incubated with either vehicle alone or 5% CSE for 24 h (A, TUNEL staining) or for the indicated time (B, agarose gel electrophoresis), they were subjected to either assay. A) Upper panels, vehicle; lower panels, 5% CSE. Left panels, DAPI staining for cell nuclei; middle panels, TUNEL staining; right panels, merge. B) Left lane, DNA size marker (1-kb ladder).

Oxidants are involved in CSE-induced cell injury

To test whether newly formed ROS contribute to nicotine- and tar-free CSE–induced cell damage, we examined the effects of antioxidants such as NAC and GSH on the CSE-induced LDH leakage, morphological changes, and TUNEL staining (Fig. 6). As shown in Fig. 6A, LDH leakage from C6 glioma cells treated with 5% CSE for 4 h was completely suppressed by treatment with 1 mM NAC or GSH. The protective effects of these agents were also observed by prevention of morphological changes and positive TUNEL staining (Fig. 6B). That is, 24-h treatment with 5% CSE induced an increase in the number of small and circular cells, which was blocked by 1 mM NAC or GSH (Fig. 6B, upper panels). Likewise, 24-h treatment with 5% CSE induced an increase in the number of TUNEL-positive cells as a marker of apoptotic cells, and the increase was suppressed by 1 mM NAC or GSH (Fig. 6B, lower panels). NAC or GSH also abolished DNA fragmentation on agarose gel electrophoresis, which was induced by 24-h or 48-h exposure to CSE (Fig. 6C). These results strongly indicate that oxidants such as ROS are involved in the CSE-induced cell damage.

$^{\cdot}OH$ derived from O_2^- induces plasma membrane damage

Next we attempted to pharmacologically characterize which type of ROS is involved in the CSE-induced plasma membrane damage. For this purpose, we examined the effects of SOD, which converts O_2^- to H_2O_2; catalase, which converts H_2O_2 to H_2O; and edaravone, which is a scavenger drug specific for $^{\cdot}OH$ (29, 30). Administration of SOD at concentrations up to 30 $U \cdot ml^{-1}$ had little effect on the increase in LDH leakage induced by 5% CSE treatment for 4 h (Fig. 7A). In contrast, the CSE-induced LDH leakage was inhibited by catalase in a concentration-dependent manner and abolished by concentrations $\geq$ 30 $U \cdot ml^{-1}$ (Fig. 7B). In the presence of a submaximal concentration (10 $U \cdot ml^{-1}$) of catalase, the catalase-resistant part of the CSE-induced LDH leakage was concentration-dependently suppressed by SOD (Fig. 7C). Notably, the CSE-induced LDH leakage was concentration-dependently inhibited by edaravone and completely suppressed at $\geq$ 30 μM (Fig. 7D). These results demonstrate that $^{\cdot}OH$ produced from O_2^- via H_2O_2 plays a major role in the CSE-induced membrane damage.

O_2^- and/or H_2O_2 induces cell death

Unlike the CSE-induced LDH leakage, the CSE-induced decrease in MTS reduction activity as an index of cell mass was virtually unaffected by edaravone (Fig. 8A). Because SOD and catalase cannot be used owing to their interfering effects on the MTS assay, we evaluated cytotoxic effects of the O_2^- generated by xanthine and xanthine oxidase (31) and of authentic H_2O_2. When the cells were incubated for 4 h with a combination of xanthine oxidase and varying concentrations of xanthine, the MTS reduction activity was inhibited with increasing concentrations of xanthine (Fig. 8B). Treatment with authentic H_2O_2 also elicited a concentration-dependent decrease in MTS reduction activity (Fig. 8C). These results suggest that CSE induces cell death via O_2^- and/or H_2O_2 rather than $^{\cdot}OH$.

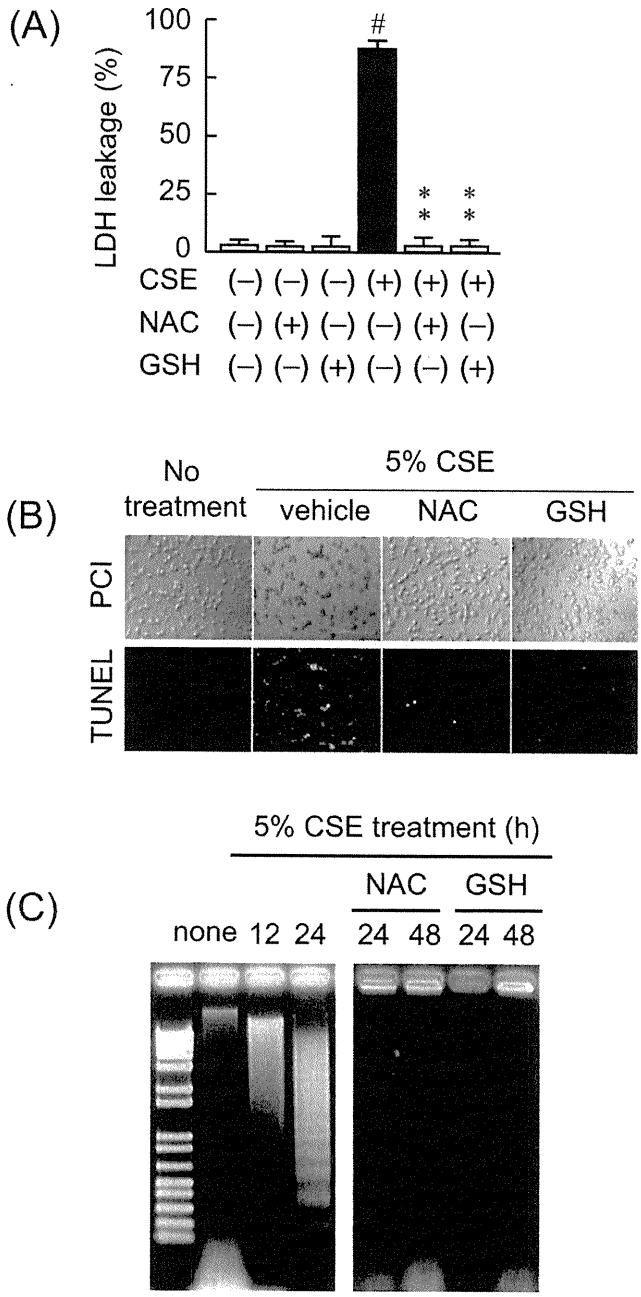

Fig. 6. Oxidants are involved in CSE-induced cytotoxicity. After C6 glioma cells were incubated with vehicle alone or 5% CSE for 24 h (A, B) or for the indicated time intervals (C), they were subjected to the LDH leakage assay (A), TUNEL staining (B), and agarose gel electrophoresis for DNA ladder (C). *N*-Acetyl-L-cysteine (NAC) or reduced glutathione (GSH) was added 10 min before the beginning of incubation with CSE. In panel A, each point represents the means ± S.E.M. of three experiments, each in triplicate. $^{\#}P < 0.01$ vs. CSE vehicle alone, $^{**}P < 0.01$ vs. CSE alone (1-way ANOVA). B) Upper panels, phase-contrast images (PCI); lower panels, TUNEL staining images on the same fields. Scale bars = 200 μm. C) Agarose gel electrophoresis. Left lane, DNA size marker (1-kb ladder).

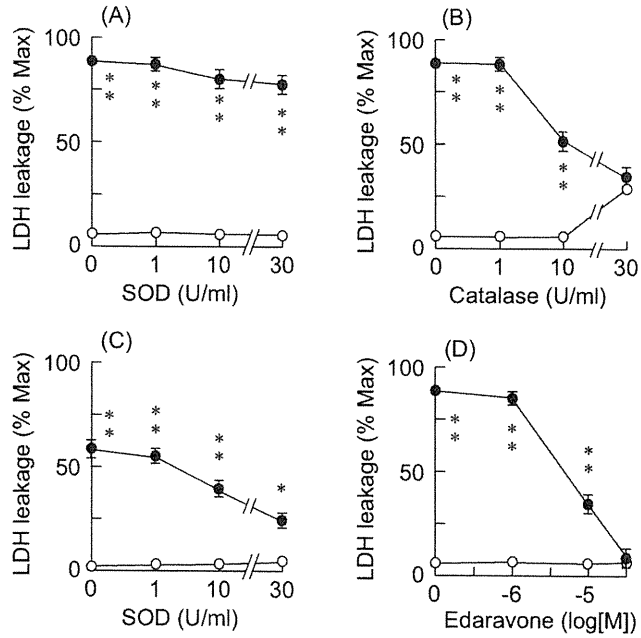

Fig. 7. Pharmacological characterization of ROS involved in plasma membrane damage of C6 glioma cells as detected by LDH leakage. C6 glioma cells were preincubated for 30 min with varying concentrations of superoxide dismutase (SOD) (A), catalase (B), SOD in combination of 10 U/ml catalase (C), or edaravone (an scavenger drug specific for ·OH) (D). After the preincubation, either vehicle (open circles) or CSE (final concentration, 5%; closed circles) was added to culture medium, 4-h incubation was performed, and LDH activity leaked into the medium was measured as described in Materials and Methods. Each point represents the means ± S.E.M. of three experiments, each in triplicate. $^{*}P < 0.05$, $^{**}P < 0.01$ vs. vehicle alone (1-way ANOVA).

CSE induces membrane damage by activating NOX via PKC

It is reported that crude CSE containing both the gas phase and the tar phase stimulates ROS production via NADPH oxidase (NOX) (15, 16). Therefore, we tested whether nicotine- and tar-free CSE can stimulate ROS production via NOX, using a NOX inhibitor (DPI) (32). Treatment of C6 glioma cells with DPI at concentrations ranging from 1 nM to 1 μM inhibited the CSE-induced LDH leakage in a concentration-dependent manner, and complete inhibition was observed at concentrations ≥ 0.1 μM (Fig. 9A).

Because DPI is reported to inhibit other ROS-generating enzymes such as nitric oxide synthase (NOS) (33) and xanthine oxidase in addition to NOX (32), we examined the effects of a NOS inhibitor, L-NAME, and a xanthine oxidase inhibitor, allopurinol. As shown in Fig. 9B, the maximally effective concentrations of L-NAME (500 μM) and allopurinol (100 μM) had little effect on the CSE-induced increase in LDH leakage. These results

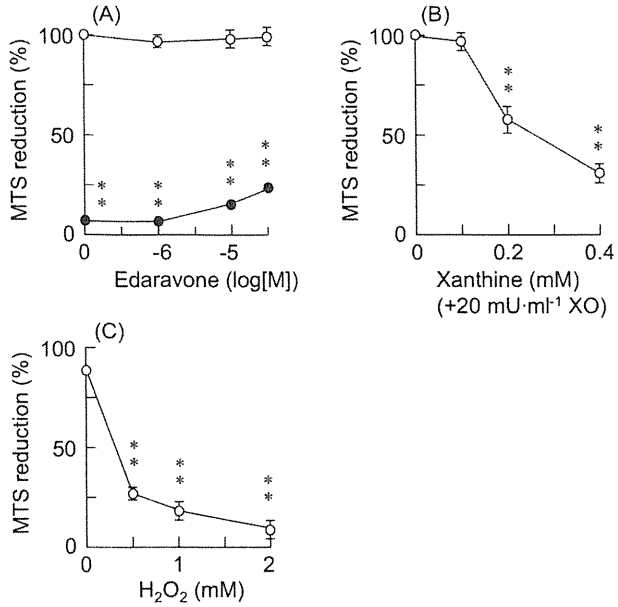

Fig. 8. Pharmacological characterization of ROS involved in reduced cell viability of C6 glioma cells as detected by MTS assay. In panel A, C6 glioma cells were incubated for 4 h with either vehicle (open circles) or 5% CSE (closed circles) in the presence of varying concentrations of edaravone. In panels B and C, the direct effects of either O_2^- (B) or H_2O_2 (C) on C6 glioma cells were examined: the cells were incubated for 4 h with 20 mU·ml^{-1} xanthine oxidase (XO) in the presence of varying concentrations of xanthine (B) or with varying concentrations of authentic H_2O_2 (C). After the incubation, MTS assay was performed as described in Materials and Methods. In panel A, C6 glioma cells were preincubated for 30 min with edaravone before the incubation. Each point represents the means ± S.E.M. of three experiments, each in triplicate. $^{**}P < 0.01$ vs. CSE vehicle (A) or vs. no treatment vehicle (B, C).

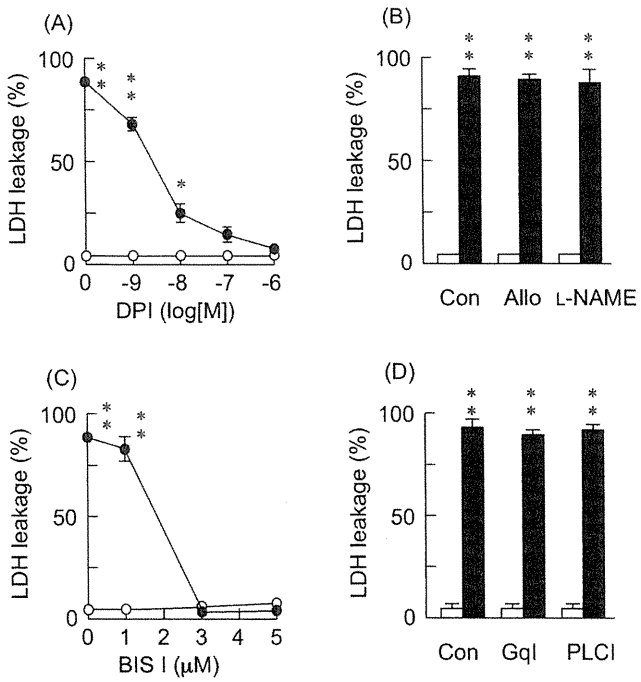

Fig. 9. Involvement of NADPH oxidase (NOX) and PKC in CSE-induced membrane damage. C6 glioma cells were preincubated for 30 min in the presence of varying concentrations of a NOX inhibitor (DPI) (A) or a PKC inhibitor (BIS I) (C). In panel B or D, the preincubation was performed in the presence of fixed concentrations of a xanthine oxidase inhibitor (Allo; allopurinol, 100 μM), a NOS inhibitor (L-NAME, 500 μM), a Gq inhibitor (GqI; YM-254893, 3 μM), or a PLC inhibitor (PLCI; U-73122, 10 μM). After the preincubation, either vehicle (open circles/bars) or CSE (final concentration, 5%; closed circles/bars) was added to the culture medium, 4-h incubation was performed, and LDH activity leaked into the medium was measured as described in Materials and Methods. Each point represents the means ± S.E.M. of three experiments, each in triplicate. $^{**}P < 0.01$ vs. CSE vehicle.

exclude the possible involvement of NOS or xanthine oxidase in the CSE-induced cell damage and indicate that NOX plays a central role in the membrane damage.

Since some types of NOX are reported to be activated by PKC (34, 35), we next examined the effects of an inhibitor of PKC, BIS I. Pretreatment with BIS I concentration-dependently inhibited the CSE (5%)-induced LDH leakage and completely suppressed it at concentrations ≥ 3 μM (Fig. 9C), indicating a major role of PKC in the CSE-induced activation of NOX.

Classical PKC isozymes are reported to be stimulated by activation of phospholipase C (PLC) via G_q protein. To examine the involvement of G_q protein and PLC, we tested the protective effects of YM-254893 (a $G_{q/11}$ protein inhibitor) (36) and U-73122 (a PLC inhibitor) on the membrane damage induced by 5% CSE. The CSE-induced LDH leakage was unaffected by pretreatment with either YM-254893 or by U-73122 (Fig. 9D), indicating that PKC is not activated by a G_q/PLC pathway.

CSE induces apoptosis via PKC/NOX-dependent and PKC/NOX-independent pathways

The CSE-induced decrease in MTS reduction activity was concentration-dependently recovered by treatment with DPI (Fig. 10A) or BIS I (Fig. 10B), and the maximal recovery was observed at concentrations ≥ 10 nM for DPI and ≥ 3 μM for BIS I. However, unlike the CSE-induced membrane damage, the maximal recovery by DPI or BIS I was partial, that is, around 50%. In accordance with the decrease in MTS reduction activity, DNA fragmentation induced by exposure to 5% CSE for 24 h was partially suppressed by the maximally effective concentration of DPI (Fig. 10C). These results taken together suggest that part of the CSE-induced apoptosis is mediated via PKC-dependent NOX activation, while the remaining part is caused independently of PKC and NOX.

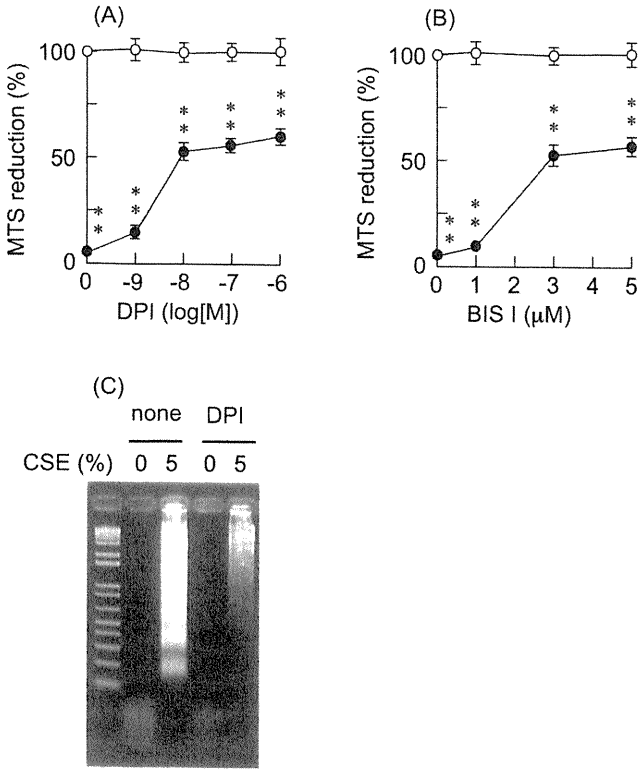

Fig. 10. Involvement of NADPH oxidase (NOX) and PKC in a decrease in cell viability and DNA fragmentation induced by CSE. After C6 glioma cells were preincubated for 30 min in the presence of varying concentrations of a NOX inhibitor (DPI) (A, C) or a PKC inhibitor (BIS I) (B), they were incubated with either vehicle (open circles) or 5% CSE (closed circles) for a further 4 h (A, B) or for 24 h (C). After the incubation, the cells were subjected to MTS reduction assay (A, B) or DNA fragmentation assay on agarose gel electrophoresis as described in Materials and Methods. In A and B, each point represents the means ± S.E.M. of three experiments, each in triplicate. $^{**}P < 0.01$ vs. CSE vehicle.

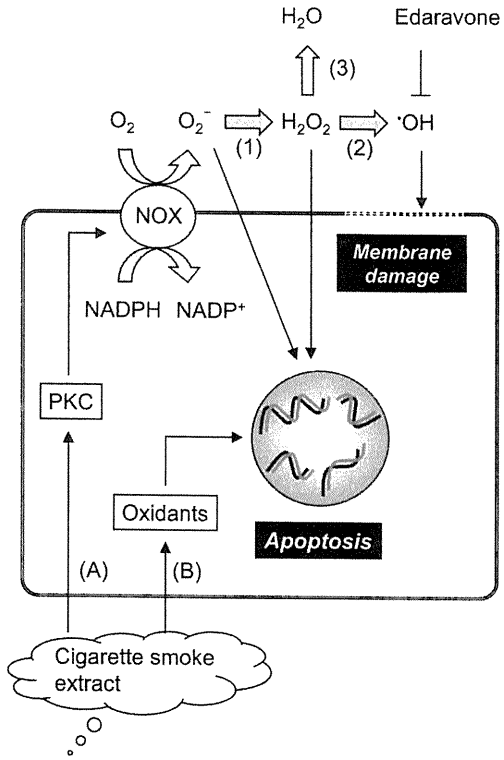

Fig. 11. Summary of the present study. Nicotine- and tar-free cigarette smoke extract generates ROS and causes plasma membrane damage and cell apoptosis through two types of mechanisms. In one mechanism (indicated by A), a stable component(s) in the CSE activates protein kinase C (PKC) directly or indirectly, which in turn stimulates NADPH oxidase (NOX) to generate $O_2^{\cdot-}$. $O_2^{\cdot-}$ is converted to H_2O_2 by superoxide dismutase (SOD), while H_2O_2 is converted to ·OH by the Fenton reaction. $O_2^{\cdot-}$ and/or H_2O_2 induce cell apoptosis including DNA fragmentation, while ·OH produces membrane damage. In the other mechanism (indicated by B), a stable component(s) in the CSE generates oxidants independently of PKC and NOX and induces cell apoptosis. Reaction (1) is catalyzed by SOD; reaction (2), by the Fenton reaction; and reaction (3), by catalase. Edaravone is a scavenger for ·OH.

Discussion

Previous investigations on the toxic effects of cigarette smoke have used either the tar phase of the cigarette smoke (22) or the crude CSE containing both the tar phase and the gas phase of the cigarette smoke (15, 16, 18 – 21). In the present study, we used the nicotine- and tar-free CSE unlike those previous works and demonstrated that 1) a stable component(s) of the CSE activated PKC, which in turn stimulated NOX to generate ROS, causing plasma membrane damage and apoptosis; 2) membrane damage and apoptosis were caused by different ROS; and 3) part of the apoptosis was caused by oxidants, which were generated independently of PKC and NOX (Fig. 11).

Characterization of CSE-induced cytotoxicity

The cell damage caused by nicotine- and tar-free CSE is categorized into three groups: 1) plasma membrane damage indexed by LDH leakage from the cells and PI uptake into the cells, 2) a decrease in the number of viable cells as indexed by MTS reduction activity, and 3) DNA fragmentation represented by positive TUNEL staining and DNA ladder on agarose gel electrophoresis.

The decrease in the number of viable cells and DNA fragmentation indicate that CSE induces cell death, which is likely to be due to apoptosis. However, there are two possible mechanisms for plasma membrane damage. One possibility is that the plasma membrane damage occurs as one aspect of the whole apoptotic process. That is, the full apoptotic program comprises two phases: pre-

necrotic phase and necrotic phase (37, 38). In the pre-necrotic phase, the apoptosing cell maintains cytoplasmic membrane integrity, and molecular alterations largely due to activated caspases produce the classical apoptotic phenotype. During this phase, phagocytosis of apoptotic cells by scavenger cells occurs and as a consequence, release of cell components is not observed. However, progression of apoptotic process to secondary necrosis can occur, when clearance by scavengers does not operate in situations such as mutation in genes required for phagocytosis or culture of cell lines: in these situations, secondary necrosis ensues, which shows characteristics similar to primary necrosis such as cytoplasmic swelling, rupture of the plasma membrane, and terminal cell disintegration with release of intracellular components (37, 38). Another possibility is that plasma membrane damage is the result of direct effects of CSE-derived ROS on the plasma membrane. Of these two possibilities, it is likely that the plasma membrane damage is caused by direct effects of ROS on the plasma membrane for the following reasons: First, the membrane damage is observed very early (approximately 1 h) following CSE exposure, when there is no DNA fragmentation as an index of apoptosis. Second, different types of ROS are responsible for the plasma membrane damage and cell apoptosis, as described below.

Characterization of ROS and the mechanism of ROS generation for membrane damage

The CSE-induced plasma membrane damage is considered to be caused by $^{\cdot}OH$ because it is reversed by edaravone, a scavenger specific for $^{\cdot}OH$. The $^{\cdot}OH$ is derived from NOX, which catalyzes the conversion of O_2 to O_2^-, based on the sensitivity of the CSE-induced damage to DPI, an inhibitor of NOX. Although DPI is reported to inhibit other ROS-generating enzymes such as NOS (33) and xanthine oxidase in addition to NOX (32), involvement of these enzymes is unlikely, based on negligible effects of specific inhibitors of these enzymes like L-NAME (a NOS inhibitor) and allopurinol (a xanthine oxidase inhibitor) on the CSE-induced cytotoxicity.

It is generally accepted that the O_2^- generated by NOX is dismutated by SOD to H_2O_2, which is converted to $^{\cdot}OH$ through a metal-catalyzed reaction known as the Fenton reaction (39). Consistent with this notion, CSE's effect on the plasma membrane was suppressed by catalase that detoxifies H_2O_2 by converting H_2O_2 to H_2O. Notably, the toxic effect was unaffected by SOD alone that converts O_2^- to H_2O_2, but it was suppressed by combined treatment with SOD and catalase that accelerates the conversion of O_2^- to H_2O via H_2O_2. The mechanism for the effectiveness of combined treatment with SOD and submaximal dose of catalase is unknown, but the effectiveness might be due to an as-yet unknown action of SOD such as catalase-like action or edaravone-like action.

Activation of NOX and O_2^- production have been reported following treatment of vascular endothelial cells with the crude CSE (15, 16). Our data clearly demonstrate that nicotine- and tar-free CSE (containing the gas phase alone) instead of the crude CSE contains stable components that have the ability to stimulate NOX and hence ROS production.

Characterization of ROS and the mechanism of ROS generation in the CSE-induced apoptosis

In contrast with membrane damage, the CSE-induced cell apoptosis is considered to involve mechanisms different from those for the plasma membrane damage. First, different species of ROS such as O_2^- or H_2O_2 (vs. $^{\cdot}OH$ for membrane damage) seem to be involved in the generation of CSE-induced apoptosis. This conclusion is based on the findings that the CSE-induced suppression of MTS reduction activity as an index of the number of viable cells is resistant to edaravone and that suppression of MTS reduction activity can be induced by either authentic H_2O_2 or O_2^- generated by the xanthine/xanthine oxidase system. Secondly, the CSE-induced apoptosis involves a NOX-independent mechanism in addition to a NOX-dependent mechanism, as evidenced by the partial sensitivity of the CSE-induced suppression of the MTS reduction activity and DNA fragmentation to DPI. The NOX-independent mechanism involves oxidants, judging from its sensitivity to antioxidants such as NAC and GSH, although its entity is at present unknown.

Activation of NOX by PKC

The NOX family consists of seven members, Nox 1 – 5 and Duox 1 – 2 (34, 35). The precise mechanism for activation of each member of the NOX family is at present not fully elucidated. Activation of some members of the NOX family such as NOX1 and NOX2 requires phosphorylation by PKC and subsequent translocation of their cytosolic subunits to the plasma membrane; activation of the other members such as NOX4 requires induction of enzyme protein; and still others such as NOX5 and Duox 1 – 2 require Ca^{2+} for activation (34, 35). The present data that activation of NOX was dependent fully on PKC strongly indicate that NOX1 and/or NOX2 are involved in the CSE-induced cytotoxicity. However, it remains to be determined which isozyme(s) of a NOX family is actually involved in the CSE-induced cytotoxicity.

Mechanism for activation of PKC by CSE

In the present study, PKC is activated by stable com-

ponents in the CSE either directly or indirectly through other molecules. The result that inhibitors of Gq protein (YM254893) and PLC (U-73122) cannot prevent the CSE-induced membrane damage excludes the possibility that PKC is activated via heptahelical Gq-protein–coupled receptors (GPCR) / PLC pathway or receptor tyrosine kinase / PLC pathway, both of which are known to be main PKC-activating systems (40). Although it is at present unknown how nicotine- and tar-free CSE activates PKC, the present findings strongly indicate that CSE contains stable components that can activate PKC to increase production of ROS via NOX. In this context, our study is an extension of previous studies (15, 16) which have shown that the crude CSE containing both the gas phase and the tar phase of cigarette smoke enhances the production of O_2^- by NOX in pulmonary artery endothelial cells without reference to the activation mechanism.

The component(s) of CSE that activates PKC and subsequently NOX is at present unknown. It is reported that the crude CSE consisting of both the gas phase and the tar phase of cigarette smoke contains a series of α,β-unsaturated aldehydes such as acrolein and crotonaldehyde, α,β-unsaturated ketones, and a number of saturated aldehydes (13). These components are stable and can react with thiol groups that might be involved in the regulation of activities of enzymes such as PKC (41, 42). A recent study suggests that acrolein, a thiol-reactive α,β-unsaturated aldehyde that is abundantly present in cigarette smoke, is actually a potent stimulator of NOX-derived O_2^- generation in pulmonary arterial endothelial cells (15, 16). At present, there are no reports that have identified such components in the nicotine- and tar-free CSE. The investigation is now under way in our laboratory that attempts to identify such active components in the nicotine- and tar-free CSE, and we have already found several molecules that induce apoptosis in a PKC/NOX-dependent or PKC/NOX-independent manner.

The concentrations of nicotine- and tar-free CSE used in the present study may be several hundred-fold higher than the concentration in the blood of a smoker that could be attained following smoking one cigarette. Even so, the cytotoxic effects could occur in various organs remote to the lung, if the chemical modification of functional molecules by components in the CSE is stable and cumulative. For example, acrolein-modified proteins have been detected in a range of diseased tissues known to sustain chronic oxidative stress, including diabetic kidneys and atherosclerotic arteries (43, 44). Therefore, after active components in CSE have been identified, it is of importance to determine their target molecules and pathophysiological significance of modification of the target molecules by the active components in CSE.

Acknowledgments

This work was supported in part by Grant-in-Aids for Scientific Research (B) from Japan Society for the Promotion of Science (JSPS) (No. 21390068 to S.M.) and for Young Scientific Research (B) from the Ministry of Education, Culture, Sports, Science, and Technology (MEXT), Japan (No. 21790236 to T.H.), and by a grant from the Smoking Research Foundation of Japan (to S.M.).

References

1 Steenland K, Thun M, Lally C, Heath C Jr. Environmental tobacco smoke and coronary heart disease in the American Cancer Society CPS-II cohort. Circulation. 1996;94:622–628.
2 Ambrose JA, Barua RS. The pathophysiology of cigarette smoking and cardiovascular disease: an update. J Am Coll Cardiol. 2004;43:1731–1737.
3 Stampfli MR, Anderson GP. How cigarette smoke skews immune responses to promote infection, lung disease and cancer. Nat Rev Immunol. 2009;9:377–384.
4 Barnes PJ, Shapiro SD, Pauwels RA. Chronic obstructive pulmonary disease: molecular and cellular mechanisms. Eur Respir J. 2003;22:672–688.
5 Shapiro SD, Ingenito EP. The pathogenesis of chronic obstructive pulmonary disease: advances in the past 100 years. Am J Respir Cell Mol Biol. 2005;32:367–372.
6 Yao H, Rahman I. Current concepts on the role of inflammation in COPD and lung cancer. Curr Opin Pharmacol. 2009;9:375–383.
7 D'Agostini F, Balansky R, Steele VE, Ganchev G, Pesce C, De Flora S. Preneoplastic and neoplastic lesions in the lung, liver and urinary tract of mice exposed to environmental cigarette smoke and UV light since birth. Int J Cancer. 2008;123:2497–2502.
8 Hecht SS, Kassie F, Hatsukami DK. Chemoprevention of lung carcinogenesis in addicted smokers and ex-smokers. Nat Rev Cancer. 2009;9:476–488.
9 Tauler J, Mulshine JL. Lung cancer and inflammation: interaction of chemokines and hnRNPs. Curr Opin Pharmacol. 2009;9:384–388.
10 Church DF, Pryor WA. Free-radical chemistry of cigarette smoke and its toxicological implications. Environ Health Perspect. 1985;64:111–126.
11 Burns DM. Cigarettes and cigarette smoking. Clin Chest Med. 1991;12:631–642.
12 Pryor WA, Stone K. Oxidants in cigarette smoke. Radicals, hydrogen peroxide, peroxynitrate, and peroxynitrite. Ann N Y Acad Sci. 1993;686:12–27;discussion 27–28.
13 Stedman RL. The chemical composition of tobacco and tobacco smoke. Chem Rev. 1968;68:153–207.
14 Pryor WA, Stone K, Zang LY, Bermudez E. Fractionation of aqueous cigarette tar extracts: fractions that contain the tar radical cause DNA damage. Chem Res Toxicol. 1998;11:441–448.
15 Jaimes EA, DeMaster EG, Tian RX, Raij L. Stable compounds of cigarette smoke induce endothelial superoxide anion production via NADPH oxidase activation. Arterioscler Thromb Vasc Biol. 2004;24:1031–1036.
16 Orosz Z, Csiszar A, Labinskyy N, Smith K, Kaminski PM, Ferdinandy P, et al. Cigarette smoke-induced proinflammatory alterations in the endothelial phenotype: role of NAD(P)H oxi-

dase activation. Am J Physiol Heart Circ Physiol. 2007;292: H130 H139.
17 Cooper KO, Witz G, Witmer C. The effects of alpha, beta-unsaturated aldehydes on hepatic thiols and thiol-containing enzymes. Fundam Appl Toxicol. 1992;19:343–349.
18 Raveendran M, Wang J, Senthil D, Wang J, Utama B, Shen Y, et al. Endogenous nitric oxide activation protects against cigarette smoking induced apoptosis in endothelial cells. FEBS Lett. 2005;579:733–740.
19 Raij L, DeMaster EG, Jaimes EA. Cigarette smoke-induced endothelium dysfunction: role of superoxide anion. J Hypertens. 2001;19:891 897.
20 Hoshino S, Yoshida M, Inoue K, Yano Y, Yanagita M, Mawatari H, et al. Cigarette smoke extract induces endothelial cell injury via JNK pathway. Biochem Biophys Res Commun. 2005;329: 58 63.
21 Hoshino Y, Mio T, Nagai S, Miki H, Ito I, Izumi T. Cytotoxic effects of cigarette smoke extract on an alveolar type II cell-derived cell line. Am J Physiol Lung Cell Mol Physiol. 2001;281: L509–L516.
22 Hellermann GR, Nagy SB, Kong X, Lockey RF, Mohapatra SS. Mechanism of cigarette smoke condensate-induced acute inflammatory response in human bronchial epithelial cells. Respir Res. 2002;3:22.
23 Yamaguchi Y, Kagota S, Haginaka J, Kunitomo M. Participation of peroxynitrite in oxidative modification of LDL by aqueous extracts of cigarette smoke. FEBS Lett. 2002;512:218–222.
24 Kunitomo M, Yamaguchi Y, Kagota S, Yoshikawa N, Nakamura K, Shinozuka K. Biochemical evidence of atherosclerosis progression mediated by increased oxidative stress in apolipoprotein E-deficient spontaneously hyperlipidemic mice exposed to chronic cigarette smoke. J Pharmacol Sci. 2009;110:354–361.
25 Frei B, Forte TM, Ames BN, Cross CE. Gas phase oxidants of cigarette smoke induce lipid peroxidation and changes in lipoprotein properties in human blood plasma. Protective effects of ascorbic acid. Biochem J. 1991;277:133–138.
26 Akaike A, Tamura Y, Sato Y, Ozaki K, Matsuoka R, Miura S, et al. Cholecystokinin-induced protection of cultured cortical neurons against glutamate neurotoxicity. Brain Res. 1991;557: 303–307.
27 Kume T, Nishikawa H, Taguchi R, Hashino A, Katsuki H, Kaneko S, et al. Antagonism of NMDA receptors by sigma receptor ligands attenuates chemical ischemia-induced neuronal death in vitro. Eur J Pharmacol. 2002;455:91 100.
28 Lecoeur H. Nuclear apoptosis detection by flow cytometry: influence of endogenous endonucleases. Exp Cell Res. 2002; 277:1 14.
29 Banno M, Mizuno T, Kato H, Zhang G, Kawanokuchi J, Wang J, et al. The radical scavenger edaravone prevents oxidative neurotoxicity induced by peroxynitrite and activated microglia. Neuropharmacology. 2005;48:283 290.
30 Higashi Y, Jitsuiki D, Chayama K, Yoshizumi M. Edaravone (3-methyl-1-phenyl-2-pyrazolin-5-one), a novel free radical scavenger, for treatment of cardiovascular diseases. Recent Pat Cardiovasc Drug Discov. 2006;1:85–93.
31 Li Y, Zhu H, Kuppusamy P, Roubaud V, Zweier JL, Trush MA. Validation of lucigenin (bis-N-methylacridinium) as a chemiluminigenic probe for detecting superoxide anion radical production by enzymatic and cellular systems. J Biol Chem. 1998;273: 2015–2023.
32 Doussiere J, Vignais PV. Diphenylene iodonium as an inhibitor of the NADPH oxidase complex of bovine neutrophils. Factors controlling the inhibitory potency of diphenylene iodonium in a cell-free system of oxidase activation. Eur J Biochem. 1992; 208:61–71.
33 Stuehr DJ, Fasehun OA, Kwon NS, Gross SS, Gonzalez JA, Levi R, et al. Inhibition of macrophage and endothelial cell nitric oxide synthase by diphenyleneiodonium and its analogs. Faseb J. 1991;5:98–103.
34 Lambeth JD. NOX enzymes and the biology of reactive oxygen. Nat Rev Immunol. 2004;4:181–189.
35 Brown DI, Griendling KK. Nox proteins in signal transduction. Free Radic Biol Med. 2009;47:1239–1253.
36 Takasaki J, Saito T, Taniguchi M, Kawasaki T, Moritani Y, Hayashi K, et al. A novel Galphaq/11-selective inhibitor. J Biol Chem. 2004;279:47438–47445.
37 Berghe TV, Vanlangenakker N, Parthoens E, Deckers W, Devos M, Festjens N, et al. Necroptosis, necrosis and secondary necrosis converge on similar cellular disintegration features. Cell Death Differ. 2010;17:922–930.
38 Silva MT. Secondary necrosis: the natural outcome of the complete apoptotic program. FEBS Lett. 2010;584:4491–4499.
39 Bergamini CM, Gambetti S, Dondi A, Cervellati C. Oxygen, reactive oxygen species and tissue damage. Curr Pharm Des. 2004;10:1611–1626.
40 Steinberg SF. Structural basis of protein kinase C isoform function. Physiol Rev. 2008;88:1341–1378.
41 Corte ED, Stirpe F. The regulation of rat liver xanthine oxidase. Involvement of thiol groups in the conversion of the enzyme activity from dehydrogenase (type D) into oxidase (type O) and purification of the enzyme. Biochem J. 1972;126:739–745.
42 Inanami O, Johnson JL, Babior BM. The leukocyte NADPH oxidase subunit p47PHOX: the role of the cysteine residues. Arch Biochem Biophys. 1998;350:36–40.
43 Suzuki D, Miyata T. Carbonyl stress in the pathogenesis of diabetic nephropathy. Intern Med. 1999;38:309–314.
44 Uchida K, Kanematsu M, Sakai K, Matsuda T, Hattori N, Mizuno Y, et al. Protein-bound acrolein: potential markers for oxidative stress. Proc Natl Acad Sci U S A. 1998;95:4882–4887.

Histamine Deficiency Decreases Atherosclerosis and Inflammatory Response in Apolipoprotein E Knockout Mice Independently of Serum Cholesterol Level

Ke-Yong Wang, Akihide Tanimoto, Xin Guo, Sohsuke Yamada, Shohei Shimajiri, Yoshitaka Murata, Yan Ding, Masato Tsutsui, Seiya Kato, Teruo Watanabe, Hiroshi Ohtsu, Ken-Ichi Hirano, Kimitoshi Kohno, Yasuyuki Sasaguri

Objective—Histamine and histamine receptors are found in atherosclerotic lesions, and their signaling and subsequent proatherogenic or proinflammatory gene expression are involved in atherogenesis. In the present study, we generated apolipoprotein E (apoE) and histamine synthesizing histidine decarboxylase double knockout (DKO) mice on a C57BL/6J (wild-type mice) background to clarify the roles of histamine in atherosclerosis.

Methods and Results—Wild-type, apoE knockout (KO), and DKO mice were fed a high-cholesterol diet to analyze hyperlipidemia-induced atherosclerosis. Compared with wild-type mice, apoE-KO mice showed increased expression of histamine and its receptors, corresponding to increased atherosclerotic lesion areas and expression of inflammatory regulators, such as nuclear factor-κB, scavenger receptors, inflammatory cytokines, and matrix metalloproteinases. Histamine deficiency after deletion of histidine decarboxylase reduced atherosclerotic areas and expression of a range of the inflammation regulatory genes, but serum cholesterol levels of DKO mice were higher than those of apoE-KO mice.

Conclusion—These results indicate that histamine is involved in the development of atherosclerosis in apoE-KO mice by regulating gene expression of inflammatory modulators, an action that appears to be independent of serum cholesterol levels. In addition to acute inflammatory response, histamine participates in chronic inflammation, such as hyperlipidemia-induced atherosclerosis, and might be a novel therapeutic target for the treatment of atherosclerosis. (***Arterioscler Thromb Vasc Biol.* 2011;31:800-807.)**

Key Words: histamine ■ histidine decarboxylase ■ hyperlipidemia-induced atherosclerosis ■ inflammation ■ matrix metalloproteinase

Recently, evidence has emerged concerning inflammatory mechanisms of the initiation and progression of atherosclerosis.[1,2] Histamine, one of the classical inflammatory mediators, is synthesized from L-histidine by a rate-limiting enzyme, histidine decarboxylase (HDC). Histamine is released from mast cells and mediates type I hypersensitivity via histamine receptor H1 (HH1R),[3] and histamine produced by enterochromaffin-like cells induces gastric acid secretion from parietal cells via histamine receptor H2 (HH2R).[4] In the field of cardiovascular pathology, accumulation of activated mast cells and histamine in the coronary adventitia has been implicated in progression of plaque rupture and acute coronary syndrome.[5–7] In addition, several epidemiological studies have reported an enhancement of atherosclerosis in the patients of allergy or increased blood histamine.[8–10] Together, these suggest a possible involvement of histamine in the pathogenesis of atherosclerosis and related disorders.

Previously, we demonstrated that HDC-knockout (KO) mice showed reduced neointimal formation induced by ligation of the carotid artery or cuff replacement of the femoral artery.[11] Because histamine stimulates smooth muscle cells (SMCs) to proliferate and SMCs predominantly express HH1R,[12] the neointimal formation, which consists of SMCs, is suggested to be an HH1R-mediated response.[11] Although ligation- or cuff-induced intimal hyperplasia mimics diffuse intimal thickening as a precursor lesion of atherosclerosis,[13] it is quite different from established atherosclerosis, in which accumulation of lipid-laden macrophages has a unique his-

Received on: August 26, 2010; final version accepted on: January 13, 2011.

From the Departments of Pathology and Cell Biology (K.-Y.W., A.T., X.G., S.Y., S.S., Y.D., Y.S.) and Molecular Biology (K.K.), School of Medicine, University of Occupational and Environmental Health, Kitakyushu, Japan; Department of Molecular and Cellular Pathology, Kagoshima University Graduate School of Medical and Dental Sciences, Kagoshima, Japan (A.T.); Kyurin Omtest Laboratory Department, Kyurin Corp, Kitakyushu, Japan (Y.M.); Departments of Pharmacology (M.T.) and Pathology and Cell Biology (S.K.), Graduate School and Faculty of Medicine, University of the Ryukyus, Okinawa, Japan; Laboratory of Pathology, Fukuoka Wajiro Hospital, Fukuoka, Japan (T.W.); Department of Applied Quantum Medical Engineering, Tohoku University, Sendai, Japan (H.O.); Department of Cardiovascular Medicine, Graduate School of Medicine, Osaka University, Osaka, Japan (K.-I.H.).

Correspondence to Yasuyuki Sasaguri, MD, PhD, Department of Pathology and Cell Biology, School of Medicine, University of Occupational and Environmental Health, 1-1 Iseigaoka, Yahatanishi-ku, Kitakyushu 807-8555, Japan. E-mail yasu3219@med.uoeh-u.ac.jp

Arterioscler Thromb Vasc Biol **is available at http://atvb.ahajournals.org** **DOI: 10.1161/ATVBAHA.110.215228**

tology. Interestingly, infiltrating macrophages in the atherosclerotic lesions express HDC as a source of histamine in human carotid arteries and the aortas of apolipoprotein E (apoE)–KO mice.[11,14,15] HDC expression in human monocytes is upregulated during macrophage differentiation, which corresponds to a switch of the histamine receptor profile from HH2R predominance in monocytes to HH1R dominance in macrophages.[16,17] Together, these results indicate that both histamine production and response is present in the cells, constituting atherosclerotic lesions and that macrophage-derived histamine could regulate atherogenic response.[18] However, the roles of histamine in the process of hyperlipidemia-induced atherosclerosis still remain unclear.

To further the examination, we generated HDC and apoE double-knockout (DKO) mice to investigate the roles of histamine in hyperlipidemia-induced atherosclerosis. The expression of inflammatory cytokines, scavenger receptors (SRs), matrix metalloproteinases (MMPs), and nuclear factor-κB (NF-κB), which regulate inflammatory response in the atherosclerotic lesions, was studied by reverse transcription–polymerase chain reaction (RT-PCR), Western blotting, and immunohistochemistry. In addition, we studied the effects of histamine on serum cholesterol.

Materials and Methods

Animals

We generated DKO mice by crossing apoE-KO mice (Jackson Laboratory, Bar Harbor, ME) with previously generated HDC-KO mice.[19] Male mice were weaned at 8 weeks of age onto a high-cholesterol diet (HcD) consisting of 1.25% cholesterol, 15% lard, and 0.5% sodium cholate (Oriental Yeast Co, Tokyo, Japan) and were maintained on this diet for 12 weeks. Another group was maintained to 23 weeks and 33 weeks of age on a normal chow diet (NcD). Wild-type (WT) C57BL/6J mice (Charles River, Yokohama, Japan) were used for control groups. Each experimental group included at least 10 mice. Animals were maintained on a 12-hour light/dark cycle. All protocols were approved by the Ethics Committee of Animal Care and Experimentation, University of Occupational and Environmental Health, and were performed according to the institutional guidelines for animal experiments and according to Law 105 and Notification 6 of the Japanese government.

Assessment of Atherosclerosis and Immunohistochemistry

The aortas were cut open longitudinally and fixed with 10% neutral buffered formalin for 24 hours. Then the aortas were stained with Oil Red O stain. *En face* images of the aortas were captured with a digital camera. Oil Red O–stained area relative to whole surface area was calculated using NIH Image software. For histological analysis, formalin-fixed and paraffin-embedded tissues were sectioned, and every 10-step sections of 1-cm length ascending aortas from the aortic valve (4-μm-thick step sections: 1500 sections/aorta) were stained with hematoxylin and eosin stain. After scanning using a virtual slide system (NanoZoomer Digital Pathology, Hamamatsu Photonics, Hamamatsu, Japan), the intima/media ratio and intimal plaque area were evaluated using NIH Image.[11,20] Immunostaining was carried out (Envision kit, Dako, Tokyo, Japan) on the paraffin sections using antibodies EPOS anti-α-smooth muscle actin (clone 1A4, ×100, Dako, Carpinteria, CA), macrophages (Mac-3 clone M3/84, ×50, BD Bioscience Pharmingen, Tokyo, Japan), HDC (rabbit polyclonal, ×100; Progen Biotechnik, Heidelberg, Germany), and histamine (rabbit polyclonal, ×100; Progen Biotechnik) as previously described.[15] Immunolocalization of NF-κB was also studies in the atherosclerotic lesions (rabbit polyclonal, ×2000, Abcam).

Lipoprotein Analysis

After mice were starved for 7 hours, blood was collected, and the serum was analyzed by high-performance liquid chromatography (Skylight Biotech, Akita, Japan).[21]

Real-Time Polymerase Chain Reaction

Expression of mRNA in the liver and aortas was quantified by real-time RT-PCR using TaqMan quantitative PCR analysis. The genes investigated and primers for PCR are listed in Table 1.

Measurement of Histamine and Monocyte Chemoattractant Protein-1 in Serum and Aortic Tissue

The aortic and serum levels of monocyte chemoattractant protein-1 (MCP-1) and histamine were measured by ELISA (R&D Systems and Immunotech, Marseille, France). The aortas were homogenized in 0.2 N $HClO_4$ buffer (100 μL/10 μg tissue), and the supernatants were collected by centrifugation (10,000*g* for 5 minutes at 4°C). After neutralization by addition of an equal volume of 1 mol/L potassium borate (pH 9.25) and measurement of protein concentration, the supernatants were subjected to ELISA.

Western Blotting

The aortic expression of class A SR (SR-A), CD36 (rabbit polyclonal, ×1000; Santa Cruz Biotechnology), and NF-κB (rabbit polyclonal, ×2000, Abcam) proteins was studied by Western blotting.

Statistical Analysis

ANOVA was applied to determine statistical differences, and a probability value of less than 0.05 was taken to be significant.

Results

General Phenotypes of DKO Mice

The body weight of apoE-KO mice was not increased, and that of WT and DKO mice was increased after NcD for 33 weeks (Supplemental Figure IA, available online at http://atvb.ahajournals.org). Both systolic and diastolic blood pressure was increased in apoE-KO mice compared with WT mice. In DKO mice, blood pressure was decreased to the level of WT mice (Supplemental Figure IB). White blood cell counts were not different among WT, apoE-KO, and DKO mice, but percentages of neutrophiles and lymphocytes were increased in apoE-KO mice. Very few basophiles were observed in the peripheral blood from WT, apoE-KO, and DKO mice (Supplemental Table I). No infectious diseases or other pathological conditions were observed during the experiments in the mice.

Serum Cholesterol Levels in DKO Mice

On feeding with NcD for 23 to 33 weeks or with HcD for 12 weeks from the age of 8 weeks, apoE-KO and DKO mice became hyperlipidemic, with increased total cholesterol (T-cho), very-low-density lipoprotein (VLDL) cholesterol, and

Table 1. Primers Used for Real-Time PCR

Gene*	Forward Primer	Reverse Primer	TaqMan Probe
CD106 (VCAM-1)	CTCATTCCCTGAAGATCCAGTAATTAA	TCAAAGGGATACACATTAGGGACTGT	TGAGTGGGCCACTTGTGCATGGG
CD36	AGGTCCTTACACATACAGAGTTCGTTATC	AACAGACAGTGAAGGCTCAAAGATG	ACTCAGGACCCCGAGGACCACACTG
CD54 (ICAM-1)	CAAACAGGAGATGAATGGTACATACG	ACCAGAATGATTATAGTCCAGTTATTTTGAG	CCATGGGAATGTCACCAGGAATGTGTACC
HDC	CAAATGTGCAGCCTGGATACC	CGTTCAATGTCCCCAAAGATG	AGTGCTCCCGAGGAACCCGACAG
HH1R	CTTTAGTGTCTTCATCCTGTGTATTGATC	GTAGCTGAAGCACGGGTCTTG	TGTCCAGCAACCCCTCCGGTACCT
HH2R	CCTTCTCTGCCATTTACCAGTTG	CATCACATCCAGGCTGGTGTAG	AGTGGAGGTTTGGCCAGGTCTTCTGC
IL1-β	TGCACTACAGGCTCCGAGATG	GTACAAAGCTCATGGAGAATATCACTTG	TGTCGGACCCATATGAGCTGAAAGCTCTC
IL1R1	AGTTAAAAGCCAGTTTTATCGCTATCC	CCCCCGATGAGGTAATTCTTG	AAATATTTTTGAGTCGGCGCATGTGCAGTTAAT
IL6	TTACACATGTTCTCTGGGAAATCG	TTGGTAGCATCCATCATTTCTTTG	TGAGAAAAGAGTTGTGCAATGGCAATTCTGAT
iNOS	GCAGTGGAGAGATTTTGCATGAC	ATGGACCCCAAGCAAGACTTG	CACCACAAGGCCACATCGGATTTCAC
LDLR	CCAAATGGCATCACACTAGATCTTT	GGTTCTCATCCTCCAAAATGGTT	TTGGGTTGATTCCAAACTCCACTCTATCTCCA
LOX-1	GTCATCCTCTGCCTGGTGTTG	AGTAAGGTTCGCTTGGTATTGTTTTAAG	TATTGTACAGTGGACACAATTACGCCA
MCP-1	GGCTCAGCCAGATGCAGTTAAC	GCCTACTCATTGGGATCATCTTG	CCCACTCACCTGCTGCTACTCATTCACC
MMP-2	CTTCACTTTCCTGGGCAACAAG	CTGCCACGAGGAATAGGCTATATC	AACCAACTACGATGATGACCGGAAGTG
MMP-3	GAGGAAATCCCACATCACCTACAG	ACCTCCTCCCAGACCTTCAAAG	ACCGGATTTGCCAAGACAGAGTGTGGAT
MMP-9	TTGAGTCCGGCAGACAATCC	CCCTGTAATGGGCTTCCTCTATG	TGATGCTATTGCTGAGATCCAGGGCG
MMP-12	GTGCCCGATGTACAGCATCTTAG	AGTCTACATCCTCACGCTTCATGTC	CGGTACCTCACTTACAGGATCTATAATTACA
PDGF-β	ACCTCGCCTGCAAGTGTGA	CTCGCTGCTCCCTGGATGT	AGTGACCCCTCGGCCTGTGACTAGAAGTC
SR-A	ACACTGCTTGATGTTCAACTCCATAC	TTTGTACACACGTTCCTCCAATTTAC	TGTCAGAGTCCGTGAATCTACAGCAAAGCAAC
SR-BI	TGGGACTTCCGGGCAGAT	GCCTCCGGGCTGAAGAAT	ACCCTTCATGACACCCGAATCCTCG
TNFR2	TGGTCTGATTGTTGGAGTGACATC	GGATTTCTCATCAGGCACATGAG	TGCATCATCCTGGTGCAGAGGAAAAAGA
18s rRNA	TaqMan Ribosomal RNA Control Reagents VIC Probe (Applied Biosystems, catalog no. 4308329)		

*iNOS indicates inducible nitric oxide synthase; PDGF, platelet-derived growth factor; TNFR, tumor necrosis factor receptor.

low-density lipoprotein (LDL) cholesterol but decreased high-density lipoprotein (HDL) cholesterol compared with WT mice (Table 2). Furthermore, compared with apoE-KO mice, DKO mice showed higher cholesterol levels in all fractions, but HDL cholesterol was moderately increased in DKO mice.

Induction of Histamine and Histamine Receptors by Hyperlipidemia

Serum histamine levels were increased in apoE-KO mice compared with WT mice during the ages of 23 to 33 weeks with NcD (Figure 1A). After 12 weeks of feeding with HcD, serum histamine levels were markedly higher than values for feeding with NcD (Figure 1B). In DKO mice, serum histamine was not detected (Figure 1A and 1B). Real-time RT-PCR showed increased HDC expression in atherosclerotic aortas of apoE-KO mice fed HcD (Figure 1C). Expression of *HH1R*, *HH2R*, and *HH3R* but not *HH4R* in atherosclerotic aortas was increased in apoE-KO mice compared with WT mice after HcD feeding, whereas it was significantly decreased in DKO mice (Figure 1D and Supplemental Figure II).

Suppression of Hyperlipidemia-Induced Atherosclerosis in DKO Mice

En face analysis demonstrated that atherosclerotic lesion area was markedly increased during the age of 23 to 33 weeks in

Table 2. HPLC Analysis of Serum Lipoproteins

	Diet	Week	WT	ApoE-KO	DKO
T-cho (mg/dL)	NcD	23	68.3±2.7	325.0±35.4*	428.2±24.8*†
	NcD	33	78.3±3.7	365.5±52.0*	496.1±37.0*†
	HcD	12	166.5±8.4	470.1±61.1*	633.5±50.8*†
VLDL (mg/dL)	NcD	23	3.9±0.6	137.7±22.8*	225.7±14.1*†
	NcD	33	6.1±0.8	208.5±34.4*	283.4±24.4*†
	HcD	12	63.7±6.1	284.8±39.1*	381.4±30.9*†
LDL (mg/dL)	NcD	23	7.5±0.3	94.5±10.3*	153.6±10.5*†
	NcD	33	9.0±0.6	107.5±17.6*	161.7±10.5*†
	HcD	12	39.2±2.6	108.4±19.9*	165.3±10.7*†
HDL (mg/dL)	NcD	23	56.9±2.0	26.2±2.8*	36.6±3.6*†
	NcD	33	63.7±2.8	28.3±1.4*	35.6±2.2*†
	HcD	12	60.9±3.1	23.0±2.1*	32.5±4.2*†

T-cho indicates total cholesterol; VLDL; very-low-density lipoprotein; LDL; low-density lipoprotein; HDL, high-density lipoprotein.

*$P<0.05$ vs WT.

†$P<0.05$ vs apoE-KO.

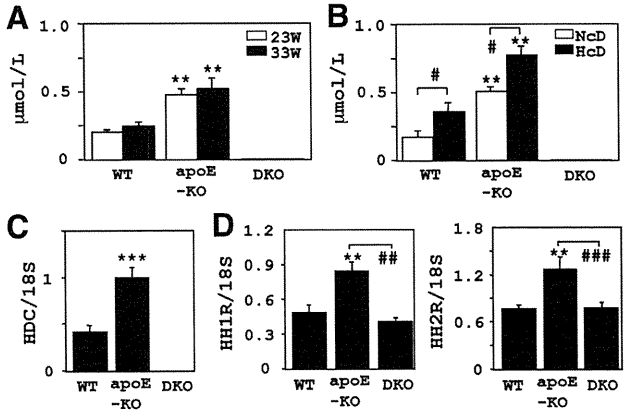

Figure 1. Serum histamine and HDC, HH1R, and HH2R expression in aortic tissue. A and B, Serum histamine was increased in apoE-KO mice but not in histamine-deficient DKO mice. From 23 to 33 weeks of age with NcD, serum histamine increased in apoE-KO mice (A), and HcD feeding for 12 weeks much increased serum histamine levels (B). C and D, Aortic expression of HDC, HH1R, and HH2R was increased in apoE-KO mice fed HcD for 12 weeks. The expression of HH1R and HH2R in DKO mice was decreased compared with apoE-KO mice. The values are presented as mean±SE. $^{*}P<0.05$, $^{**}P<0.01$, $^{***}P<0.001$ vs WT mice; $\#\#P<0.05$, $\#\#\#P<0.001$.

apoE-KO mice fed NcD, whereas it was much less in DKO mice (40% of apoE-KO mice) (Figure 2A). After mice were fed HcD for 9 or 12 weeks, atherosclerotic lesion area in DKO mice was also 40% of that of apoE-KO mice (Figure

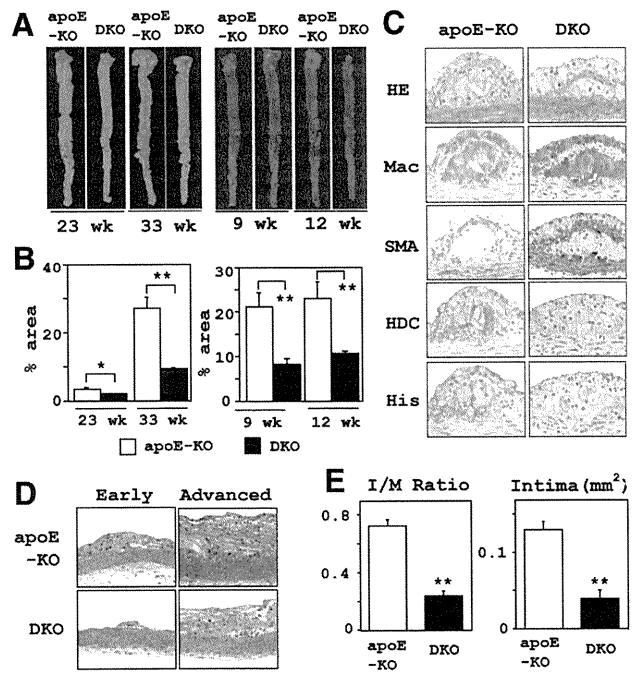

Figure 2. Quantitative analysis of hyperlipidemia-induced atherosclerosis. A, Oil Red O–stained atherosclerotic lesions in NcD-fed (for 23 and 33 weeks) and HcD-fed (9 and 12 weeks) mice. B, The atherosclerotic areas stained with Oil Red O stain were decreased in DKO mice fed NcD and HcD. The values are presented as mean±SE. $^{*}P<0.05$, $^{**}P<0.01$ vs apoE-KO mice. C and D, Representative microphotographs of the aortic lesions. E, Intima to media ratio (I/M ratio) in NcD-fed mice (33 weeks) evaluated from serial sections of the aorta. The values are presented as mean±SE. $^{**}P<0.01$ vs apoE-KO mice. HE indicates hematoxylin and eosin; Mac, Mac-3; SMA, α-SMA; His, histamine.

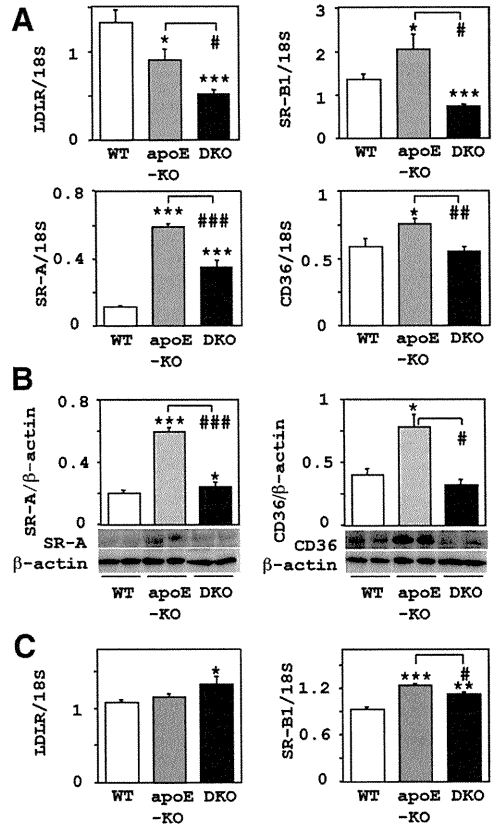

Figure 3. Expression of LDLR, SR-BI, and SRs in atherosclerotic aortas. A, Expression of LDLR and SRs in the aortas was analyzed in WT and KO mice fed HcD for 12 weeks. The expression of these genes was downregulated in DKO mice compared with apoE-KO mice. B, SR-A and CD36 expression in protein levels was studied by Western blotting. The expression levels in protein were correlated with those in mRNA. C, In the liver, SR-BI expression was decreased in DKO mice, but that of LDLR was increased in DKO mice compared with apoE-KO mice. Values were normalized by 18S rRNA expression (RT-PCR) or β-actin (Western blotting) expression and are presented as mean±SE. $^{*}P<0.05$, $^{**}P<0.01$, $^{***}P<0.001$ vs WT mice; $\#P<0.05$, $\#\#P<0.01$, $\#\#\#P<0.001$ vs apoE-KO mice.

2B). The atherosclerotic lesions of apoE-KO mice included Mac-3-positive macrophages (foam cells) and a lesser number of α-smooth muscle actin–positive SMCs. The macrophages were positive for HDC and histamine in apoE-KO mice (Figure 2C). In addition to the Mac-3-positive macrophages, a few CD3-positive T lymphocytes infiltrated in the atherosclerotic intima (data not shown). The T cell counts were increased in apoE-KO and DKO mice compared with WT mice, but they were not different between apoE-KO and DKO mice (Supplemental Table II).

Because mast cells in HDC-KO mice are decreased in number and show abnormal morphology and reduced granular content,[19] the mast cells in the atherosclerotic aortas were studied by toluidine blue stain. Mast cells were not observed in the atherosclerotic intima, but a few cells were detected in the adventitia, and no significant differences in these cell numbers were noted among WT, apoE-KO, and DKO mice (data not shown).

In 33-week-old mice fed NcD, intima/media ratio and intimal lesion area were significantly reduced by 60% in DKO mice

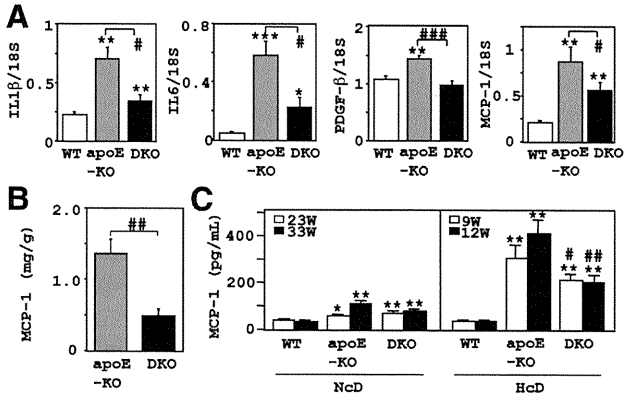

Figure 4. Expression of inflammatory factors in atherosclerotic aortas. A, Expression of inflammatory factors in the aorta was analyzed in WT, apoE-KO, and DKO mice fed HcD for 12 weeks. These genes expression were increased in apoE-KO mice but decreased in DKO mice. B, Aortic MCP-1 content in DKO mice was lower than that in apoE-KO mice in 12 weeks of HcD. C, Serum MCP-1 was increased in apoE-KO and DKO mice fed NcD from 23 to 33 weeks of age. After HcD feeding for 9 and 12 weeks, serum MCP-1 of both apoE-KO and DKO mice were increased compared with that of WT mice. Tissue MCP-1 was normalized by tissue weight. The mRNA expression was normalized by 18S rRNA expression and is presented as mean±SE. *$P<0.05$, **$P<0.01$, ***$P<0.001$ vs WT; #$P<0.05$, ##$P<0.01$ vs apoE-KO mice.

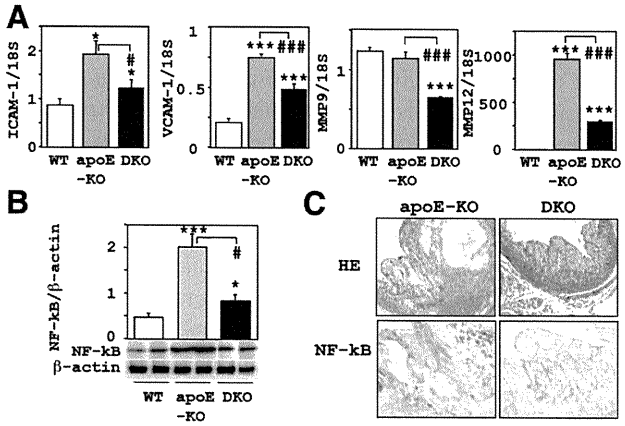

Figure 5. Expression of adhesion molecules, MMPs, and NF-κB. Expression of ICAM-1, VCAM-1, and MMPs in the aorta in WT, apoE-KO, and DKO mice fed HcD for 12 weeks. Values were normalized by 18S rRNA expression and are presented as mean±SE. A, ICAM-1 and VCAM-1 expression was increased in atherosclerotic aortas in apoE-KO mice and decreased in DKO mice. MMP expression was also increased in atherosclerotic plaques of apoE-KO mice, except for MMP-9, and was decreased in DKO mice. The expression of NF-κB was studied by Western blotting (B) and immunohistochemistry (C). In apoE-KO mice, NF-κB expression was increased and localized in the nuclei of the macrophages. Both expression and nuclear localization were decreased in DKO mice. *$P<0.05$, **$P<0.01$, ***$P<0.001$ vs WT mice; #$P<0.05$, ##$P<0.01$ vs apoE-KO mice.

compared with apoE-KO mice (Figure 2D and 2E). Mice fed HcD for 9 to 12 weeks had similar results (data not shown).

Expression of SRs and LDL Receptor in the Liver and Aortas in DKO Mice

Real-time RT-PCR revealed that expression of LDL receptor (LDLR) was decreased in both apoE-KO and DKO compared with WT mice but was further decreased in DKO mice compared with apoE-KO mice. SRs, including SR-A,[22] SR-BI,[23] CD36,[24] and lectin-like oxidized LDLR-1 (LOX-1)[25] were increased in apoE-KO mice fed HcD for 12 weeks. The expression of these SRs genes was significantly downregulated in DKO mice compared with apoE-KO mice (Figure 3A and Supplemental Figure III). The levels of protein expression of SR-A and CD36 were correlated to those of mRNA expression (Figure 3B). In the liver, mRNA expression of *SR-BI* was moderately decreased in DKO mice, but that of *LDLR* was increased in DKO mice compared with apoE-KO mice (Figure 3C).

Suppression of Inflammatory Response in Atherosclerotic Aortas of DKO Mice

Expression of inflammatory cytokines or growth factors and their receptors, such as tumor necrosis factor receptor, interleukin-1 receptor (*IL1R*), *IL-1β*, *IL-6*, platelet-derived growth factor β chain, and *MCP-1*, was increased in apoE-KO mice compared with WT mice and decreased in DKO mice (Figure 4A and Supplemental Figure III). In addition, serum and aortic tissue MCP-1 protein levels were significantly decreased in DKO mice compared with apoE-KO mice (Figure 4B and 4C). Expression of mRNAs of intercellular adhesion molecule-1 (ICAM-1) and vascular cell adhesion molecule-1 (VCAM-1) was increased in atherosclerotic aortas of apoE-KO mice but significantly decreased in DKO mice (Figure 5A). Inducible nitric oxide synthase, expression of which is regulated by HH1R signaling in vascular SMCs,[26] was enhanced in apoE-KO mice and reduced in DKO mice (Supplemental Figure III).

Decreased Expression of MMPs in Atherosclerotic Aortas in DKO Mice

Expression of MMPs, which participate in the remodeling of atherosclerotic intima,[20,27,28] was increased in atherosclerotic plaques of apoE-KO mice, except for *MMP-9* after feeding with HcD for 12 weeks. In particular, *MMP-12* expression, which was hardly detected in the normal aortic tissue from WT mice, was markedly enhanced in apoE-KO mice. All the *MMP* mRNA expression investigated was significantly decreased in DKO mice (Figure 5A and Supplemental Figure III).

Decreased Expression and Nuclear Localization of NF-κB in Atherosclerotic Aortas in DKO Mice

One of the key regulators of inflammation, transcriptional factor NF-κB expression in the aortas, was evaluated by Western blotting and immunohistochemistry. In the atherosclerotic aortas of mice fed HcD for 12 weeks, expression was markedly increased in apoE-KO mice and decreased in DKO mice (Figure 5B). As shown by immunostaining, nuclear localization of NF-κB in the infiltrated macrophages, detected in apoE-KO mice, was decreased in DKO mice (Figure 5C).

Discussion

In the present study, we demonstrated that serum and aortic histamine contents and histamine receptor expression increased as hyperlipidemia-induced atherosclerosis developed in apoE-KO mice. In histamine-deficient DKO mice, atherosclerotic lesion was significantly attenuated despite the higher cholesterol levels. The expression of a range of proatherogenic cytokines, SRs, adhesion molecules, and MMPs in the aortas was reduced in DKO mice. Expression and activation of NF-κB, one of the key inflammatory regulators, was also decreased in DKO mice. Therefore, these results indicate that histamine promotes atherosclerosis independently of serum cholesterol levels but depending on gene regulation of inflammatory response.

Regulation of Atherosclerosis and Serum Lipid by Histamine

In both liver and atherosclerotic aortas, SR-BI expression were reduced in DKO compared with apoE-KO mice. HDL cholesterol receptor SR-BI regulates reverse cholesterol transport from peripheral atherosclerotic lesions to the liver, and deletion of SR-BI in apoE-KO mice accelerates proatherogenic hypercholesterolemia and atherosclerosis.[23,29] Therefore, decreased expression of SR-BI is responsible in part for the increased cholesterol levels in DKO mice. In contrast, LDLR expression in the liver was moderately increased and that in the aortas was decreased in DKO mice. Because LDLR is expressed predominantly in the liver and LDLR-deficient mice show proatherogenic lipid profile because of reduced hepatic clearance of LDL and very-low-density lipoprotein,[30,31] it is probable that LDLR-mediated clearance of serum cholesterol would not, at least, be impaired in DKO mice.

In contrast, HDL cholesterol levels in DKO mice were higher than those in apoE-KO mice. The higher serum HDL cholesterol levels might partly participate in the reduction of atherosclerosis in DKO mice. Although the net effect of histamine deficiency on apoE-KO mice is attenuation of atherosclerosis with increased very-low-density lipoprotein, LDL, and HDL cholesterol, the exact mechanism(s) by which histamine regulates cholesterol metabolism is still unknown. Recently, however, we suggested that hepatic cholesterol accumulation is regulated by histamine signaling in the liver,[32] and therefore histamine actions mediated through histamine receptors expressed in tissues, including the artery and liver, probably regulate cholesterol metabolism.

On the other hand, SR-A, CD36, LOX-1, and SR-BI, which are the receptors for oxidized LDL and mainly expressed in atherosclerotic lesions to promote atherosclerosis,[22–25] were decreased in DKO mice. Partially supporting the present results, LOX-1 expression in monocytes is upregulated by histamine-mediated signal through HH2R.[17] Therefore, suppressed influx of modified LDL in aortas by histamine deficiency is implicated in reduced atherosclerosis progression in DKO mice in spite of increased serum cholesterol levels. In fact, atherosclerosis, which is enhanced in LDLR-KO or apoE-KO mice, is reduced by deficiency of LOX-1, SR-A, and CD36 expression.[33,34] Histamine is able to enhance cholesterol influx in peripheral tissues, resulting in the accumulation of cholesterol in lipid-laden cells in the aortas to accelerate atherosclerosis.

Regulation of Inflammatory Response by Histamine

Our study showed that proatherogenic cytokines and other molecules (such as IL-1β, IL-6, platelet-derived growth factor-BB, inducible nitric oxide synthase, and MCP-1) which regulate inflammatory response in the atherosclerotic lesions, were markedly decreased along with attenuation of hyperlipidemia-induced atherosclerosis in DKO mice. Because influx of modified LDL into the atherosclerotic lesions also accelerates the inflammatory responses to the progress of atherosclerosis,[35,36] the decreased cholesterol influx contributes to the decreased inflammation to reduce atherosclerotic lesions in DKO mice.

Among those inflammatory factors, our previous studies showed histamine regulation of MCP-1 in relation to atherogenesis.[15,37,38] Histamine stimulates monocytes to express MCP-1 and its receptor chemokine (c-c motif) receptor 2 (CCR2), and it stimulates endothelial cells to upregulate ICAM-1 and VCAM-1 expression,[37] which are upregulated at atherosclerosis-prone sites in apoE-KO mice.[39] The expression of MCP-1 is also upregulated by granulocyte-macrophage colony-stimulating factor, which enhances the production of histamine via HDC expression of monocytes.[15,38] These data suggest that histamine modulates monocyte migration from peripheral blood via upregulation of MCP-1/CCR2 and adhesion molecules and that histamine is involved in an inflammatory network in the atherosclerotic lesion.[18] Actually, in the present study, the serum and aortic MCP-1 expression in DKO mice was significantly lower than that in apoE-KO mice. In addition, the aortic expression of endothelial and monocytic adhesion molecules, including ICAM-1 and VCAM-1, was induced in apoE-KO mice but significantly reduced in DKO mice. Because the increased expression of MCP-1 and adhesion molecules plays a central role in the progression and destabilization of established atherosclerosis in apoE-KO mice,[40] these data indicate that the antiatherogenic nature of DKO mice could, at least partially, be attributed to the downregulation of histamine-induced expression of MCP-1 and adhesion molecules.

Regulation of MMP Expression and Intimal Remodeling by Histamine

Transgenic expression or KO of MMP genes has been very often introduced in apoE-KO mice or another animal to investigate the relation between atherosclerosis and arterial matrix degradation.[41–43] Of special interest, the effects of MMP-9 and MMP-12 are well studied because of its elastolytic activity to destroy the arterial media for the progression of atherosclerosis. Indeed, we previously reported that MMP-12 plays an essential role in the invasion of macrophages into hypercholesterolemia-induced atherosclerotic foci in MMP-12 transgenic rabbits by disruption of elastic fibers.[20] The current data concerning MMPs indicate that

histamine participates in tissue remodeling in hyperlipidemia-induced atherosclerosis via the expression of MMP-2, -3, -9, and -12. Although histamine is not able to directly induce these expression of these MMPs in cultured macrophages and SMCs (data not shown), the expression of MMPs is regulated by a complicated inflammation network including histamine in the atherosclerotic lesions.[18] It is of note that oxidized LDL–induced expression of MMP-2 and -9 in atherosclerotic lesions of LDLR-KO mice is mediated though activation of LOX-1,[44] because our previous study showed that histamine upregulates LOX-1 expression in monocytes.[17] The histamine-LOX-1-MMP axis may be present in atherosclerotic lesions to modulate extracellular matrix metabolism.

Regulation of NF-κB Signaling in Inflammatory Responses by Histamine

NF-κB signaling is critical for atherogenesis because it regulates vascular inflammatory responses, and activated NF-κB has demonstrated in atherosclerotic lesions.[45,46] Importantly, all the genes whose expression was decreased in DKO mice are targets of the transcriptional factor NF-κB in the atherosclerotic lesion.[45] Because the expression and nuclear localization of NF-κB were decreased in DKO mice, these data indicate that histamine regulates NF-κB signaling in atherogenesis.

In conclusion, the present study indicates that the inflammatory response induced by histamine is an important regulator of atherosis induced by high serum cholesterol. Therefore, histamine could be a relevant therapeutic target in the treatment of atherosclerosis.

Acknowledgments

The authors thank Dr Masao Kimoto in the Faculty of Medicine, Saga University, for his critical suggestions and also to thank Hiroko Isakai, Hana Nishimura, Naoko Une, and Tomoko Shima for their expert technical assistance.

Sources of Funding

This work was supported in part by research grants from the Smoking Research Foundation (to A.T.) and by Grant-in-Aid 20590416 from the Japanese Ministry of Education, Science and Culture, Tokyo, Japan (to A.T. and Y.S.).

Disclosures

No competing financial interests exist.

References

1. Zelcer N, Tontonoz P. Liver X receptors as integrators of metabolic and inflammatory signaling. *J Clin Invest*. 2006;116:607–614.
2. Hansson GK. Inflammation, atherosclerosis, and coronary artery disease. *N Engl J Med*. 2005;352:1685–1695.
3. White MV. The role of histamine in allergic diseases. *J Allergy Clin Immunol*. 1990;86:599–605.
4. Brzozowski T, Konturek PC, Konturek SJ, Kwiecień S, Pajdo R, Drozdowicz D, Ptak A, Pawlik M, Hahn EG. Involvement of gastrin in gastric secretory and protective actions of *N*-α-methyl histamine. *J Physiol (Paris)*. 2001;95:89–98.
5. Forman MB, Oates JA, Robertson D, Robertson RM, Roberts LJ II, Virmani R. Increased adventitial mast cells in a patient with coronary spasm. *N Engl J Med*. 1985;313:1138–1141.
6. Laine P, Kaartinen M, Penttila A, Panulä P, Paavonen T, Kovanen PT. Association between myocardial infarction and the mast cells in the adventitia of the infarct-related coronary artery. *Circulation*. 1999;99:361–369.
7. Steffel J, Akhmedov A, Greutert H, Lüscher TF, Tanner FC. Histamine induces tissue factor expression: implications for acute coronary syndromes. *Circulation*. 2005;112:341–349.
8. Knoflach M, Kiechl S, Mayr A, Willeit J, Poewe W, Wick G. Allergic Rhinitis, Asthma, and Atherosclerosis in the Bruneck and ARMY Studies. *Arch Intern Med*. 2005;165:2521–2526.
9. Iribarren C, Tolstykh IV, Eisner MD. Are patients with asthma at increased risk of coronary heart disease? *Int J Epidemiol*. 2004;33:743–748.
10. Clejan S, Japa S, Clemetson C, Hasabnis SS, David O, Talano JV. Blood histamine is associated with coronary artery disease, cardiac events and severity of inflammation and atherosclerosis. *J Cell Mol Med*. 2002;6:583–592.
11. Sasaguri Y, Wang KY, Tanimoto A, Tsutsui M, Ueno H, Murata Y, Kohno Y, Yamada S, Ohtsu H. Role of histamine produced by bone marrow-derived vascular cells in pathogenesis of atherosclerosis. *Circ Res*. 2005;96:974–981.
12. Takagishi T, Sasaguri Y, Nakano R, Arima N, Tanimoto A, Fukui H, Morimatsu M. Expression of the histamine H1 receptor gene in relation to atherosclerosis. *Am J Pathol*. 1995;146:981–988.
13. Nakashima Y, Fujii H, Sumiyoshi S, Wight TN, Sueishi K. Early human atherosclerosis: accumulation of lipid and proteoglycans in intimal thickenings followed by macrophage infiltration. *Arterioscler Thromb Vasc Biol*. 2007;27:1159–1165.
14. Higuchi S, Tanimoto A, Arima N, Xu H, Murata Y, Hamada T, Makishima K, Sasaguri Y. Effects of histamine and interleukin-4 synthesized in arterial intima on phagocytosis by monocytes/macrophages in relation to atherosclerosis. *FEBS Lett*. 2001;505:217–222.
15. Murata Y, Tanimoto A, Wang K-Y, Tsutsui M, Sasaguri Y, Corte FD, Matsushita H. Granulocyte macrophage–colony stimulating factor increases the expression of histamine and histamine receptors in monocytes/macrophages in relation to arteriosclerosis. *Arterioscler Thromb Vasc Biol*. 2005;25:430–435.
16. Wang KY, Arima N, Higuchi S, Shimajiri S, Tanimoto A, Murata Y, Hamada T, Sasaguri Y. Switch of histamine receptor expression from H2 to H1 during differentiation of monocytes into macrophages. *FEBS Lett*. 2000;473:345–348.
17. Tanimoto A, Murata Y, Nomaguchi M, Kimura S, Arima N, Xu H, Hamada T, Sasaguri Y. Histamine increases the expression of LOX-1 via H2 receptor in human monocytic THP-1 cells. *FEBS Lett*. 2001;508:345–349.
18. Tanimoto A, Sasaguri Y, Ohtsu H. Histamine network in atherosclerosis. *Trends Cardiovasc Med*. 2006;16:280–284.
19. Ohtsu H, Tanaka S, Terui T, Hori Y, Makabe-Kobayashi Y, Pejler G, Tchougounova E, Hellman L, Gertsenstein M, Hirasawa N, Sakurai E, Buzás E, Kovács P, Csaba G, Kittel Á, Okada M, Hara M, Mar L, Numayama-Tsuruta K, Ishigaki-Suzuki S, Ohuchi K, Ichikawa A, Falus A, Watanabe T, Nagy A. Mice lacking histidine decarboxylase exhibit abnormal mast cells. *FEBS Lett*. 2001;502:53–56.
20. Yamada S, Wang KY, Tanimoto A, Fan J, Shimajiri S, Kitajima S, Morimoto M, Tsutsui M, Watanabe T, Yasumoto K, Sasaguri Y. Matrix metalloproteinase 12 accelerates the initiation of atherosclerosis and stimulates the progression of fatty streaks to fibrous plaques in transgenic rabbits. *Am J Pathol*. 2008;172:1419–1429.
21. Usui S, Hara Y, Hosaki S, Okazaki M. A new on-line dual enzymatic method for simultaneous quantification of cholesterol and triglycerides in lipoproteins by HPLC. *J Lipid Res*. 2002;43:805–814.
22. Gough PJ, Greaves DR, Suzuki H, Hakkinen T, Hiltunen MO, Turunen M, Herttuala SY, Kodama T, Gordon S. Analysis of macrophage scavenger receptor (SR-A) expression in human aortic atherosclerotic lesions. *Arterioscler Thromb Vasc Biol*. 1999;19:461–471.
23. Acton S, Rigotti A, Landschulz KT, Xu S, Hobbs HH, Krieger M. Identification of scavenger receptor SR-B1 as a high density lipoprotein receptor. *Science*. 1996;271:518–520.
24. Park YM, Febbraio M, Silverstein RL. CD36 modulates migration of mouse and human macrophages in response to oxidized LDL and may contribute to macrophage trapping in the arterial intima. *J Clin Invest*. 2009;119:136–145.
25. Sawamura T, Kume N, Aoyama T, Moriwaki H, Hoshikawa H, Aiba Y, Tanaka T, Miwa S, Katsura Y, Kita T, Masaki T. An endothelial receptor for oxidized low-density lipoprotein. *Nature*. 1997;386:73–77.

26. Tanimoto A, Wang KY, Murata Y, Kimura S, Nomaguchi M, Nakata S, Tsutui M, Sasaguri Y. Histamine upregulates the expression of inducible nitric oxide synthase in human intimal smooth muscle cells via histamine H1 receptor and NF-κB signaling pathway. *Arterioscler Thromb Vasc Biol.* 2007;27:1556–1561.
27. Sasaguri Y, Yanagi H, Nagase H, Nakano R, Fukuda S, Morimatsu M. Collagenase production by immortalized human aortic endothelial cells infected with simian virus 40. *Virchows Arch B Cell Pathol Incl Mol Pathol.* 1991;60:91–97.
28. Sasaguri Y, Murahashi N, Sugama K, Kato S, Hiraoka K, Satoh T, Isomoto H, Morimatsu M. Development-related changes in matrix metalloproteinase expression in human aortic smooth muscle cells. *Lab Invest.* 1994;71:261–269.
29. Trigatti B, Rayburn H, Vinals M, Braun A, Miettinen H, Penman M, Hertz M, Schrenzel M, Amigo L, Rigotti A, Krieger M. Influence of the high density lipoprotein receptor SR-BI on reproductive and cardiovascular pathophysiology. *Proc Natl Acad Sci U S A.* 1999;96:9322–9327.
30. Ishibashi S, Brown MS, Goldstein JL, Gerard RD, Mammer RE, Herz J. Hypercholesterolemis in low density lipoprotine receptor knockout mice and its reversal by adenovirus-mediated gene delivery. *J Clin Invest.* 1993;92:883–893.
31. Osono Y, Woollett LA, Herz J, Dietschy JM. Role of the low density lipoprotein receptor in the flux of cholesterol through the plasma and across the tissue of the mouse. *J Clin Invest.* 1995;95:1124–1132.
32. Wang KY, Tanimoto A, Yamada S, Guo X, Ding Y, Watanabe T, Watanabe T, Kohno K, Hirano K, Tsukada H. Sasaguri Y. Histamine regulation in glucose and lipid metabolism via histamine receptors: model for nonalcoholic steatohepatitis in mice. *Am J Pathol.* 2010;177:713–723.
33. Mehta JL, Sanada N, Hu CP, Chen J, Dandapat A, Sugawara F, Satoh H, Inoue K, Kawase Y, Jishage K, Suzuki H, Yakeya M, Schnackenberg L, Berger R, Hermonat PL, Thomas M, Sawamura T. Deletion of LOX-1 reduces atherogenesis in LDLR knockout mice fed high cholesterol diet. *Circ Res.* 2007;100:1634–1642.
34. Manning-Tobin JJ, Moore KJ, Seimon TA, Bell SA, Sharuk M, Alvarez-Leite JI, de Winther MP, Tabas I, Freeman MW. Loss of SR-A and CD36 activity reduces atherosclerotic lesion complexity without abrogating foam cell formation in hyperlipidemic mice. *Arterioscler Thromb Vasc Biol.* 2009;29:19–26.
35. Khovidhunkit W, Kim MS, Memon RA, Shigenaga JK, Moser AH, Feingold KR, Grunfeld C. Effects of infection and inflammation on lipid and lipoprotein metabolism: mechanisms and consequences to the host. *J Lipid Res.* 2004;45:1169–1196.
36. Bensinger SJ, Tontonoz P. Integration of metabolism and inflammation by lipid-activated nuclear receptors. *Nature.* 2008;454:470–477.
37. Kimura S, Wang KY, Tanimoto A, Murata Y, Nakashima Y, Sasaguri Y. Acute inflammatory reactions caused by histamine via monocytes/macrophages chronically participate in the initiation and progression of atherosclerosis. *Pathol Int.* 2004;54:465–474.
38. Tanimoto A, Murata Y, Wang KY, Tsutsui M, Kohno K, Sasaguri Y. Monocyte chemoattractant protein-1 expression is enhanced by granulocyte-macrophage colony-stimulating factor via jak2-stat5 signaling and inhibited by atorvastatin in human monocytic U937 cells. *J Biol Chem.* 2008;283:4 643–4651.
39. Nakashima Y, Raines EW, Plump AS, Breslow JL, Ross R. Upregulation of VCAM-1 and ICAM-1 at atherosclerosis-prone sites on the endothelium in the apoE-deficient mouse. *Arterioscler Thromb Vasc Biol.* 1998;18:842–851.
40. Ni W, Egashira K, Kitamoto S, Kataoka C, Koyanagi M, Inoue S, Imaizumi K, Akiyama C, Nishida KI, Takeshita A. New anti-monocyte chemoattractant protein-1 gene therapy attenuates atherosclerosis in apolipoprotein E-knockout mice. *Circulation.* 2001;103:2096–2101.
41. Luttun A, Lutgens E, Manderveld A, Maris K, Collen D, Carmeliet P, Moons L. Loss of matrix metalloproteinase-9 or matrix metalloproteinase-12 protects apolipoprotein E-deficient mice against atherosclerotic media destruction but differentially affects plaque growth. *Circulation.* 2004;109:1408–1414.
42. Gough PJ, Gomez IG, Wille PT, Raines EW. Macrophage expression of active MMP-9 induces acute plaque disruption in apoE-deficient mice. *J Clin Invest.* 2006;116:59–69.
43. Kuzuya M, Nakamura K, Sasaki T, Cheng XW, Itohara S, Iguchi A. Effect of MMP-2-deficiency on atherosclerotic lesion formation in apoE-deficient mice. *Arterioscler Thromb Vasc Biol.* 2006;26:1120–1125.
44. Hu C, Dandapat A, Sun L, Chen J, Marwali MR, Romeo F, Sawamura T, Mehta JL. LOX-1 deletion decreases collagen accumulation in atherosclerotic plaque in low-density lipoprotein receptor knockout mice fed a high-cholesterol diet. *Cardiovasc Res.* 2008;79:287–293.
45. de Winther MPJ, Kanters E, Kraal G, Hofker MH. Nuclear factor κB signaling in atherogenesis. *Arterioscler Thromb Vasc Biol.* 2005;25:904–914.
46. Brand K, Page S, Rogler G, Bartsch A, Brandl R, Knuechel R, Page M, Kaltschmidt C, Bauerle PA, Neumeier D. Activated transcriptional factor nuclear factor-κB is present in the atherosclerotic lesion. *J Clin Invest.* 1996;97:1715–1722.

Highlighted Paper selected by Editor-in-Chief

Roles of Histamine in Exercise-Induced Fatigue: Favouring Endurance and Protecting against Exhaustion

Fukie Niijima-Yaoita,*[,a] Masahiro Tsuchiya,[b] Hiroshi Ohtsu,[c] Kazuhiko Yanai,[d] Shunji Sugawara,[e] Yasuo Endo,[e] and Takeshi Tadano[a]

[a] *Department of Pharmacology, Tohoku Pharmaceutical University; 4–4–1 Komatsushima, Aoba-ku, Sendai 981–8558, Japan:* [b] *Department of Aging and Geriatric Dentistry, Graduate School of Dentistry, Tohoku University; 4-1 Seiryo-machi, Aoba-ku, Sendai 980-8575, Japan:* [d] *Department of Pharmacology, Graduate School of Medicine, Tohoku University;* [c] *Department of Molecular Regulation, Graduate School of Dentistry, Tohoku University; 4–1 Seiryo-machi, Aoba-ku, Sendai 980–8575, Japan: and* [e] *Department of Applied Quantum Medical Engineering, School of Engineering, Tohoku University; 6-6-01-2 Aoba, Aramaki-aza, Aoba-ku, Sendai 980–8575, Japan.*

Received August 17, 2011; accepted October 25, 2011; published online November 4, 2011

Exercise necessitates a large supply of O_2 and nutrients and rapid removal of CO_2 and waste products. Histamine is a regulator of the microcirculation (which performs these exchanges), suggesting a possible involvement of histamine in exercise. Histamine is released from either mast cells or non-mast cells. In the latter, histamine is newly formed *via* the induction of histidine decarboxylase (HDC) in response to an appropriate stimulus, and it is released without being stored. Here, in mice, we examined the role of histamine or HDC induction in exercise. Prolonged walking (PW) (in a cylindrical cage turned electrically) increased HDC mRNA and HDC activity in quadriceps femoris muscles. Mice given a histamine H1-receptor antagonist [fexofenadine (peripherally acting) or pyrilamine (peripherally and centrally acting)] or an irreversible HDC inhibitor (α-fluoromethylhistidine) displayed less PW endurance than control mice. Ranitidine (H2-receptor antagonist) tended to reduce endurance. Other histamine-receptor (H3 and H4) antagonists had no significant effects on endurance. Mice deficient in HDC or histamine H1-receptors displayed markedly less endurance than control mice, and HDC activity in the quadriceps femoris of H1-deficient mice was rapidly elevated by PW. Fexofenadine significantly reduced the muscle levels of nitric oxide (NO) metabolites and glycogen after PW. The results support the ideas that (i) histamine is involved in protecting against exercise-induced fatigue or exhaustion, (ii) histamine exerts its protective effect *via* H1 receptors and the ensuing production of NO in skeletal muscle, and (iii) histamine is provided, at least in part, by HDC induction in skeletal muscles during prolonged exercise.

Key words exercise; histidine decarboxylase; histamine receptor; nitric oxide; skeletal muscle

Although it is common knowledge that during exercise (*i.e.* repeated muscle contraction), there is an increased need for nutrients and O_2 to be supplied to skeletal muscles and for waste metabolites and CO_2 to be removed from them, the detailed mechanisms responsible for the support of such vascular functions remain unclear.

Histamine dilates precapillary arterioles and increases capillary permeability.[1–3] Thus, histamine, if provided appropriately within or to skeletal muscles, may help to support the supply of O_2 and nutrients and the removal of CO_2 and waste products. The vasodilating effect of histamine on arterioles is largely induced by stimulation of histamine H1 receptors and the ensuing production of nitric oxide (NO).[3–5]

It is widely known that histamine is stored within mast cells and basophils. It is also known that the histamine-forming enzyme, histidine decarboxylase (HDC), is a typical adaptive enzyme induced in response to a variety of stimuli.[6–10] The histamine newly formed *via* HDC induction is released without being stored,[7–11] and it has been suggested that histamine from this source is involved both in the regulation of the microcirculation[8,9] and in anabolic processes during rapid cell growth.[7]

Interestingly, prolonged walking (PW) (or other prolonged physical exercise) induces HDC in mouse skeletal muscles,[12–15] and the elevation of HDC activity persists for several hours after the exercise ends.[14] It has also been shown that training decreases the magnitude of the exercise-stimulated HDC induction.[13,14] It has also been shown that in humans, histamine H1 and H2 receptors are involved in mediating post-exercise hyperemia in skeletal muscles and/or post-exercise hypotension.[16–18] Therefore, a plausible hypothesis is that histamine may play a role in exercise endurance, possibly by reducing muscle fatigue.

In the present study, on mice, we employed antagonists of histamine receptors, an inhibitor of HDC, and mice deficient either in HDC or in histamine H1 receptors to examine the roles played by histamine and HDC in exercise endurance.

MATERIALS AND METHODS

Animals C57BL/6 mice were purchased from Japan CLEA (Tokyo, Japan). Histamine H1-receptor knockout (H1-KO) mice (C57BL/6 background) were originally produced by Inoue and colleagues.[19] HDC-KO mice (C57BL/6 background) were established by Ohtsu *et al.*[20] H1-KO and HDC-KO mice were bred in the laboratory of Sugawara (Department of Molecular Immunology, Graduate School of Dentistry, Tohoku University). The mice (male) used for the present experiments were 7 to 8 weeks old. Body weight of the mice at the time of experiments was about 24 g for the other mice. All mice were allowed standard food pellets (LabMR Stock; Nihon Nosan Inc., Yokohama, Japan) and tap water *ad libitum* in an air-conditioned room at 23±1°C and 55±5% relative humidity with a standard 12 h light and12 h dark cycle (lights on at 07:00 a.m.). All experiments complied with the Guidelines for Care and Use of Laboratory Animals issued by Tohoku Pharmaceutical

* To whom correspondence should be addressed. e-mail: niijima@tohoku-pharm.ac.jp

University.

Reagents DL-α-Monofluoromethylhistidine (FMH, an irreversible inhibitor of HDC) was a gift from Dr. Kollonitsch of Merck Sharp and Dohme Research Laboratories (Rahway, NJ, U.S.A.).[21] Fexofenadine, pyrilamine, ranitidine, and thioperamide were purchased from Sigma Chemical Co. (St. Louis, MO, U.S.A.). Fexofenadine was suspended in saline containing 0.5% Tween 80. All other reagents were dissolved in saline. The above reagents were injected intraperitoneally at 0.1 mL per 10 g body weight. JNJ-7777120, which was provided by Johnson & Johnson Pharmaceutical Research and Development, LLC, (San Diego, CA, U.S.A.),[22] was suspended in saline and injected intraperitoneally at 0.2 mL per 10 g body weight. In all experiments, saline or vehicle was injected at the same volume and same timing as the solutions of test drugs. The doses employed in the present study were within the ranges widely used in experiments on mice and rats.[22—25]

Prolonged Walking (PW) and PW-Endurance Forced walking at room temperature (23±1°C) was imposed on mice for a time indicated in each experiment, as described previously.[14] Briefly, mice were put into a cylindrical cage (36 cm diameter, 36 cm width), the wall of which was made of stainless steel rods (2 mm diameter, 1 cm apart). The cage was turned around a horizontal axis by an electric motor, the speed being indicated in each experiment. For the first 1—2 h of the experiment, most mice followed the rotation of the cage by walking on the steel rods using their fore- and hind-feet or by hanging from the rods rather than by walking. However, some mice spent this period revolving to higher positions then jumping to lower position. After this period, some mice became unable to follow the speed, as evidenced by alternate periods of walking and sliding, and later there was falling from the hanging position, with the number of mice falling becoming greater as walking was prolonged. In endurance experiments, whenever we observed falling or signs of distress (*e.g.*, unsuccessful attempts to walk at the required speed), the mouse was immediately removed from the cage by a blinded investigator. In such experiments, the number of mice still walking was recorded at various time-points.

Assay of HDC Activity For the assay of HDC activity, mice were sacrificed by decapitation without anesthesia after the indicated duration of PW. Then, their quadriceps femoris muscles and brains were removed and stored at −80°C until assay. HDC activity was assayed using our previously published method[26] with a slight modification.[14,27] Briefly, each tissue sample (less than 250 mg) was put into a cooled Teflon tube together with phosphorylated cellulose (50—100 mg) and 2.5 mL of ice-cold 0.02 M phosphate buffer (pH 6.2) containing pyridoxal 5′-phosphate (20 μM) and dithiothreitol (200 μM). This mixture was then homogenized using an Ultra Turrax homogenizer (Janke and Kunkel Co., Berlin, Germany). The supernatant obtained after centrifugation of the homogenate (10000 ***g*** for 15 min at 4°C) was used as the enzyme solution. The histamine in the tissues was bound to the phosphorylated cellulose and was removed almost completely from the enzyme solution by the centrifugation. Reaction mixture (1 mL) containing the enzyme solution was incubated at 37°C for 16 h with histidine (1 mM). After the enzyme reaction had been terminated by adding 2 mL of 0.5 M $HClO_4$, the histamine formed during the incubation was separated by chromatography on a small phosphorylated cellulose column, then quantified fluorometrically.[26] HDC activity was expressed as n mol of histamine formed during a 1 h period of incubation by the enzyme contained in 1 g (wet weight) of each tissue (nmol/h/g).

Quantitative Real-Time Polymerase Chain Reaction (PCR) Analysis of HDC mRNA Using Trizol reagent (Invitrogen, CA, U.S.A.), total RNA was extracted from the quadriceps femoris muscles of mice were sacrificed by decapitation without anesthesia at the time-points indicated in the relevant experiment. cDNA was prepared with the aid of a SuperScript first-strand synthesis system (Invitrogen) and subjected to quantitative real-time PCR analysis using iQ SYBR green (Bio-Rad, Hercules, CA, U.S.A.). Gene-specific primers were designed using DNAStar software (DNASTAR, Inc., Madison, WI, U.S.A.). The primers for '*HDC*' expression were 5′-CCG AGG GGG AGG TGT CTT AC-3′ (forward) and 5′-CGA GCC GAG CGT TCA GG-3′ (reverse) and for '*endothelial nitric oxide synthase (eNOS)*' were 5′-GGG CGG GGA GCG ACT ACT-3′ (forward) and 5′-GCA GCA GCT TTG GCA TCT TCT-3′ (reverse). The internal control primers for '*EF1α1*' were F5′-ATT CCG GCA AGT CCA CCA CAA-3′ and R5′-CAT CTC AGC AGC CTC CTT CTC AAA C-3′. The PCR profile was 3 min at 95°C for initial melting; 20 s at 95°C, 30 s at 58°C for 45 cycles; 30 s at 95°C for 1 cycle; and then 1 min at 55°C followed by stepwise temperature increases from 55 to 95°C to generate the melt curve. Standard curves and PCR efficiencies were determined for each primer set using control cDNA and a 10-fold dilution series ranging from 1000 to 1 ng/mL. Relative expression levels of 'HDC' were calculated as a function of '*EF1α1*' expression.[28]

Measurement of NO Metabolites Since NO is rapidly converted to the stable metabolites NO_2^- and/or NO_3^- (largely to the latter), the production of NO can be evaluated by measuring these metabolites.[29] Mice were sacrificed by decapitation without anesthesia and quadriceps femoris muscles were quickly removed and immediately homogenized in 2 vol of methanol. The homogenate was centrifuged at 10000 ***g*** for 10 min at 4°C. The supernatant was used for the analysis of NO metabolites (NO_2^- and NO_3^-). They were separated by a high performance liquid chromatography (HPLC), which includes systems converting NO_3^- to NO_2^-, converting NO_2^- to a chromophoric azo product by the Griese reaction,[29] and measuring its absorbance at 540 nm (ENO-20, EICOM, Japan). The results of the analyses are expressed as nmol/g tissue.

Measurement of Muscle Glycogen Muscle glycogen was measured by a conventional method,[30] using an enzymatic glucose-determining kit (Glucose-CII-test-Wako; Wako Pure Chemical Industries, Osaka, Japan).

Data Analysis Data from endurance tests were analyzed by Kaplan–Meier analysis using the log-rank test (GraphPad Prism, GraphPad Software Inc., San Diego, CA, U.S.A.). Experimental values are given as means±standard deviation (S.D.). The statistical significance of the difference between two means was evaluated using a Student's unpaired *t* test. For analyzing multiple mean values, Tukey–Kramer or Fisher's protected least significant difference (PLSD) *post hoc* test was employed after analysis of variance (ANOVA) using the Statview-J 5.0 computer program (SAS Institute, Inc., U.S.A.). In these tests, p values less than 0.05 were considered to indicate significance.

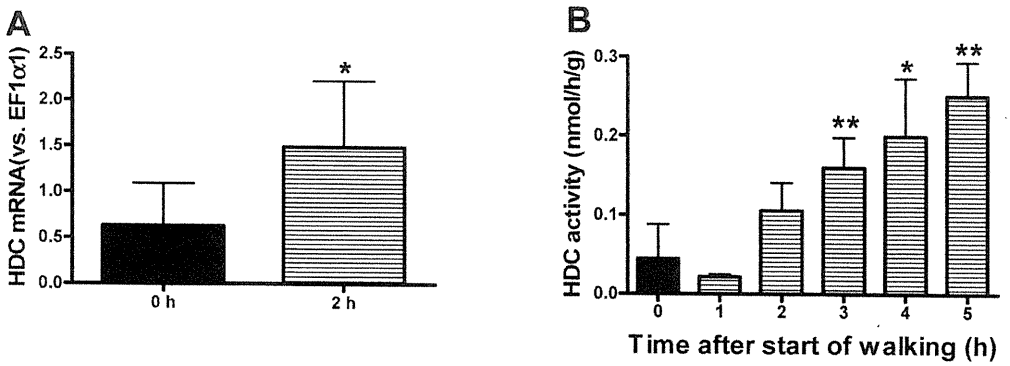

Fig. 1. Induction of HDC in Quadriceps Femoris Muscles of C57BL/6 Mice Performing PW at a Speed of 9 m/min

(A) Induction of HDC mRNA. Muscles were taken 2 h after the start of PW and analyzed for HDC mRNA. Each value represents the mean±S.D. from 6 mice. *$p<0.05$ *vs.* time 0. (B) Time course of the induction of HDC activity. Muscles were taken at the time-points indicated. Although 3 h after the start of PW, some mice became unable to follow the required speed (repeatedly walking, then sliding), their muscles were used for measurement. The mice capable of following the speed were left in the cylindrical cage for the remainder of the periods of PW. Each value represents the mean±S.D. from 4 mice. *$p<0.05$ and **$p<0.01$ *vs.* time 0.

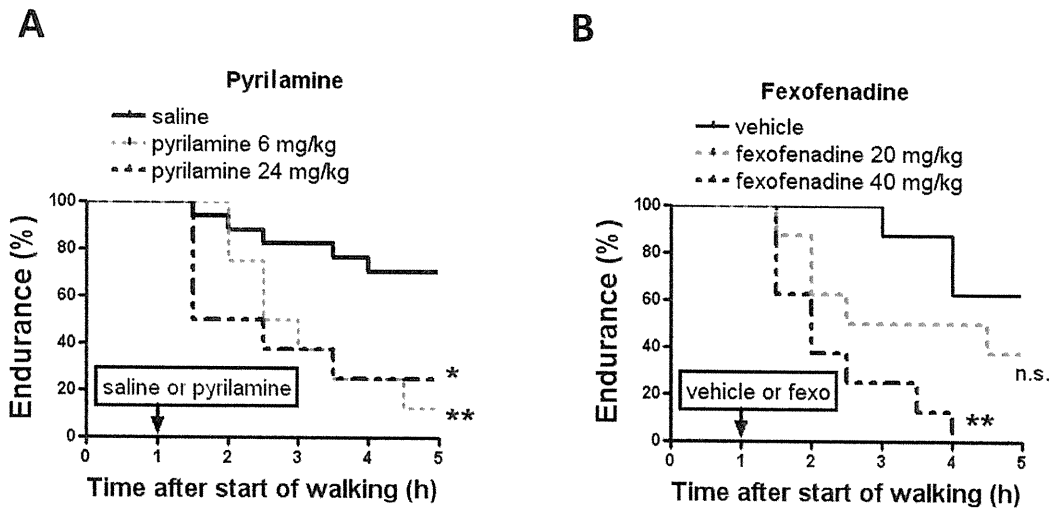

Fig. 2. Effects of the H1-Receptor Antagonists Pyrilamine (A) and Fexofenadine (B) on PW-Endurance of C57BL/6 Mice

PW was carried out at a speed of 9 m/min. Mice were given (A) saline or pyrilamine, or (B) vehicle or fexofenadine at the indicated dose at 1 h after the start of PW, and PW-endurance monitoring was continued for the next 4 h. n=8—17 for each group. *$p<0.05$ or **$p<0.01$ *vs.* mice injected with saline or vehicle.

RESULTS

Induction of HDC by PW in C57BL/6 Mice On the basis of preliminary experiments, PW was imposed on mice at a speed of 9 m/min, except where otherwise noted. PW elevated both HDC mRNA and HDC activity in the quadriceps femoris muscle in C57BL/6 mice (Fig. 1). The HDC activity was greater at longer durations of PW. On the other hand, HDC activities in the brain were not different between time 0 (0.59±0.05 nmol/h/g, n=5) and time 5 h after the start of PW (0.62±0.05 nmol/h/g, n=5). Thus, in the following experiments, we focused on the HDC in the quadriceps femoris muscles alone.

Effects of Histamine H1-Receptor Antagonists on PW-Endurance Pyrilamine and fexofenadine are histamine H1-receptor antagonists, and it is known that while the former acts on both peripheral and central receptors, the latter acts predominantly on peripheral receptors.[31] As shown in Figs. 2A and B, each of these antagonists (injected 1 h after the start of PW) dose-relatedly reduced the PW-endurance abilities of C57BL/6 mice. In other words, these drugs appeared to promote fatigue during PW.

Effects of Histamine H2-, H3-, and H4-Receptor Antagonists on PW-Endurance Ranitidine, thioperamide, and JNJ-7777120 are antagonists of histamine H2-, H3-, and H4-receptors, respectively. Ranitidine (injected 1 h after the start of PW) tended (non-significantly) to reduce PW-endurance in C57BL/6 mice (Fig. 3A). When the data from C57BL/6 were statistically analyzed at 2 h (but not at other time-points) after the start of PW, the differences between the saline group and the two groups given ranitidine were significant. However, C57BL/6 mice did not exhibit any significant changes in PW-endurance in response to thioperamide (injected 1 h after the start of PW) (Fig. 3B). JNJ-7777120 had no significant effects, either, in C57BL/6 mice under any conditions tested (various doses and injection timings) (data not shown).

Effects of an Irreversible HDC Inhibitor on PW-Endurance α-Monofluoromethylhistidine (FMH) is an irreversible (or suicide) HDC inhibitor.[22] FMH strongly inhibits HDC in various tissues in mice at or around the dose used in the present study.[32,33] As shown in Fig. 4, FMH potently promoted exercise-induced fatigue in C57BL/6 mice.

PW-Endurance and HDC Induction in HDC-KO and H1-KO Mice In the experiments described above, PW

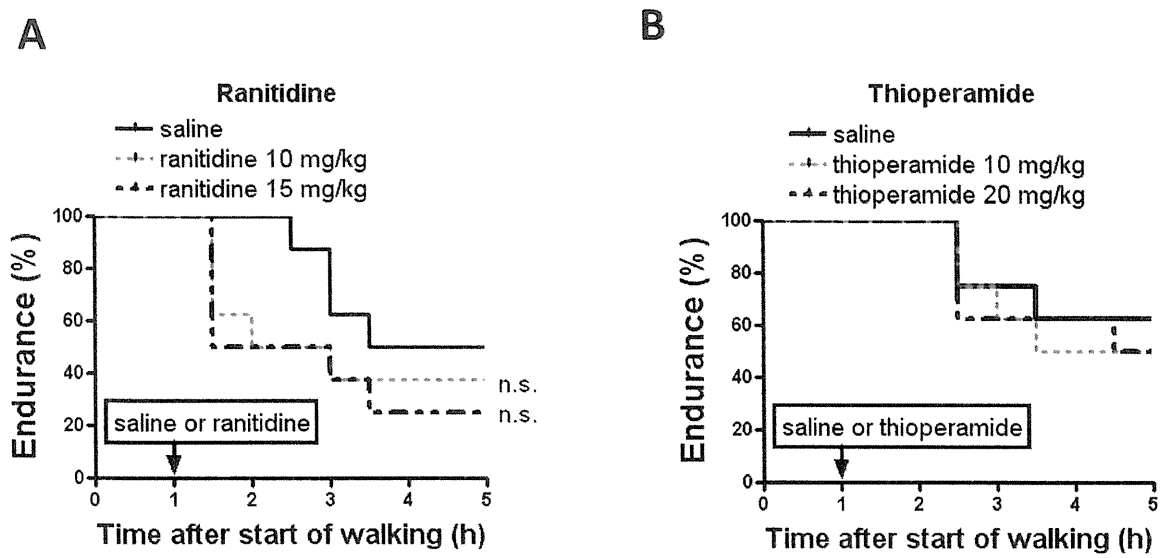

Fig. 3. Effects of Ranitidine (A) and Thioperamide (B) on PW-Endurance of C57BL/6 Mice Performing PW at a Speed of 9 m/min

Mice were given (A) saline or ranitidine or (B) saline or thioperamide at the indicated dose at 1 h after the start of PW, and PW-endurance monitoring was continued for the next 4 h. n=8—11 for each group.

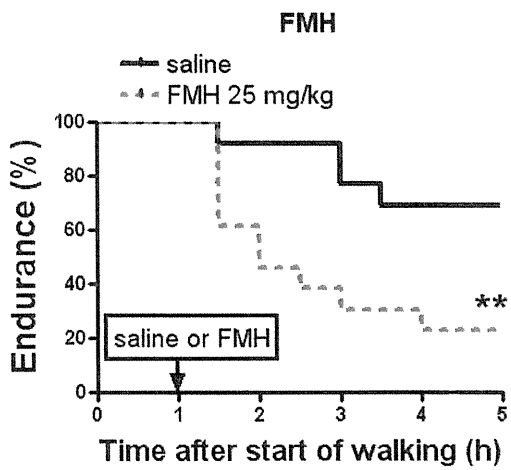

Fig. 4. Effects of FMH, an Irreversible HDC Inhibitor, on PW-Endurance of C57BL/6 Mice Performing PW at a Speed of 9 m/min

Saline or FMH (25 mg/kg) was given at 1 h after the start of PW, and PW-endurance monitoring was continued for the next 4 h. n=13 for each group. **$p<0.01$ *vs.* mice injected with saline.

was imposed on the mice at a speed 9 m/min. However, in preliminary experiments we noted that neither HDC-KO nor H1-KO mice could follow this speed. We therefore compared PW-endurance abilities between these KO mice and their control wild-type (WT) mice (C57BL/6) using a speed of 7.5 m/min. As shown in Figs. 5A and B, these KO mice displayed markedly less PW-endurance than the WT mice. Interestingly, HDC activity in the quadriceps femoris muscles of H1-KO mice, but not in those of the WT mice, was significantly elevated as early as 90 min after the start of PW (Fig. 5C).

Effects of Fexofenadine on Muscle NO Production and Glycogen Content As described in Introduction, the microcirculation is important in exercise, and histamine is a regulator of the microcirculation. Histamine-induced arteriolar vasodilation is largely mediated by histamine H1-receptors and the subsequent production of NO.[3—5] In addition, muscle glycogen is an important energy source for exercise. Thus, we examined the effects of fexofenadine on the PW-induced production of NO and levels of glycogen in quadriceps femoris muscles.

Effects on NO Production As shown in Figs. 6A and B, fexofenadine did not affect the resting levels of NO metabolites. Unexpectedly, these resting levels were similar to those measured after 3 h PW (possibly, their rates of release from and production by the muscle were similar to each other).

However, after 3 h PW their levels were significantly lower in the fexofenadine group (this result was unexpected because eNOS is said to be a constitutive enzyme). These results suggest not only that PW activated eNOS, but also that it induced this enzyme to some extent *via* stimulation of peripheral histamine H1-receptors.

Effects on Glycogen Levels After 3 h PW, the level of muscle glycogen tended to be decreased, and it was significantly lower (*vs.* vehicle) in the fexofenadine group (Fig. 6D). This lower level in fexofenadine-treated mice may be causally related to their reduced PW-endurance (Fig. 2).

DISCUSSION

The results obtained from WT C57BL/6 mice, HDC-KO, and H1-KO mice may be summarized as follows. (i) PW increased HDC mRNA and HDC activity in quadriceps femoris muscles. (ii) Mice given one of two types of histamine H1-receptor antagonist (peripherally acting or both peripherally and centrally acting) or an irreversible HDC inhibitor exhibited less endurance than control mice. (iii) Mice deficient in HDC or histamine H1-receptors also exhibited less PW-endurance than control mice. (iv) The increase in HDC activity induced by PW was greater in the muscles of H1-deficient mice than in those of their WT controls. (v) Mice given the peripheral H1 antagonist fexofenadine displayed significantly reduced muscle levels of NO metabolites and glycogen after 3 h walking (*vs.* vehicle-treated mice), although this drug did not affect their resting levels. We discuss these findings in the following

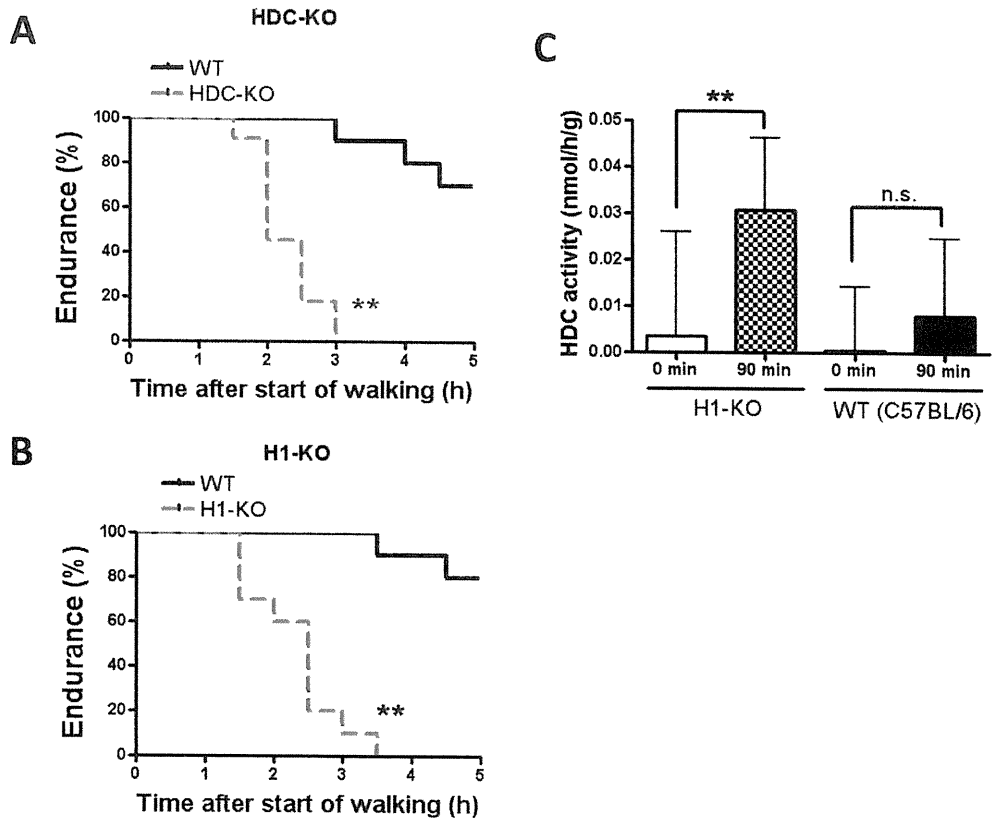

Fig. 5. PW-Endurance of HDC-KO and H1-KO Mice, and HDC Induction in such Mice

(A, B) PW, at a speed of 7.5 m/min, was monitored for up to 5 h. n=10—11 for each group. **p<0.01 *vs.* the relevant WT control. (C) HDC induction in the quadriceps femoris muscle at 90 min after the start of PW in H1-KO and their WT control mice. Each value represents the mean±S.D. from 8—11 mice. **p<0.01 *vs.* time 0 min.

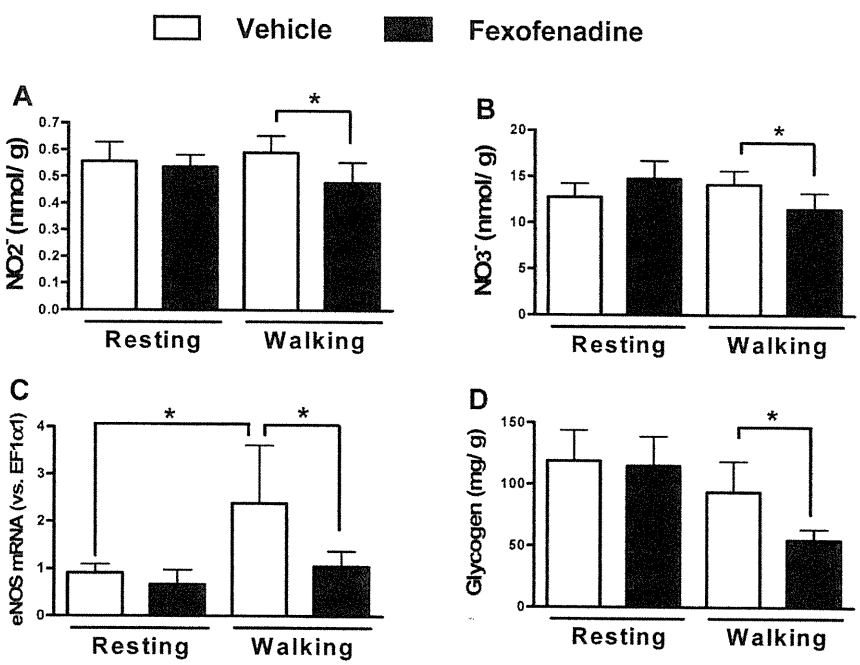

Fig. 6. Effects of Fexofenadine on eNOS, NO_2^-, NO_3^-, and Glycogen Levels in Quadriceps Femoris Muscles in C57BL/6 Mice

In the resting group, muscles were taken 2 h after an injection of vehicle or fexofenadine (40 mg/kg) without PW. In the walking group, vehicle or fexofenadine was given at 1 h after the start of PW (9 m/min), and muscles were taken after an additional 2 h PW. Although some mice in this group became unable to follow the required speed (repeatedly walking, then sliding), their muscles were used for measurement. n=6 or 7 for each group. *p<0.05 between the indicated two groups.

paragraphs.

When discussing the present data, we need to consider whether the observed effects on endurance abilities could reflect effects on the skeletal muscles themselves or on other organs (central nervous system, lung, heart, liver, *etc.*). PW induces HDC not only in skeletal muscles (quadriceps femo-